Journal of Zhejiang University-SCIENCE A 2025 26(9):853-875
www.jzus.zju.edu.cn; www.springer.com/journal/11582
E-mail: jzus_a@zju.edu.cn

Review

https://doi.org/10.1631/jzus.A2500067

Check for updates

In-process cutting temperature measurement for ultra-precision machining: a comprehensive review and future perspectives

Shiquan LIU, Yuqi DING, Kaiyang XIA, Hui LI, Liang AN, Zhongwei LI, Yuan-Liu CHEN✉

State Key Laboratory of Fluid Power and Mechatronic Systems, Zhejiang University, Hangzhou 310058, China

Abstract: With the widespread adoption of ultra-precision machining (UPM) in manufacturing, accurately monitoring the temperature within micro-scale cutting zones has become crucial for ensuring machining quality and tool longevity. This review comprehensively evaluates modern in-process cutting temperature measurement methods, comparing conventional approaches and emerging technologies. Thermal conduction-based and radiation-based measurement paradigms are analyzed in terms of their merits, limitations, and domain-specific applicability, particularly with regard to the unique challenges involving micro-scale cutting zones in UPM. Special emphasis is placed on micro-scale sensor-integrated tools and self-sensing tools that enable real-time thermal monitoring at cutting edges. Furthermore, we explore thermal monitoring and management techniques for atomic and close-to-atomic scale manufacturing (ACSM), as well as the transformative potential of emerging technologies like artificial intelligence (AI), internet of things (IoT), and data fusion for machining temperature measurement. This review may serve as a reference for UPM cutting temperature measurement research, helping foster the development of optimized process control technologies.

Key words: Cutting temperature measurement; Ultra-precision machining (UPM); In-process monitoring; Smart sensors; Micro-scale cutting zones

1 Introduction

Ultra-precision machining (UPM) technology has become a cornerstone in modern manufacturing, playing an indispensable role in various fields including aerospace, precision instruments, microelectronics, and optics (Brinksmeier et al., 2004; Gao et al., 2013; Fang et al., 2017). The escalating demands for machining accuracy, surface quality, and specific material properties across industries have rendered traditional mechanical processing technologies inadequate for meeting such requirements. Consequently, UPM technology has emerged as an effective method for nano-scale manufacturing (Jawahir et al., 2011; Fan et al., 2022; Gao et al., 2023).

UPM not only necessitates equipment with exceptional precision and stability, but also effective heat control during cutting processes (Fang et al., 2022). Cutting temperature is a critical process parameter in UPM, directly influencing factors such as tool wear patterns, cutting force distributions, workpiece surface quality, and dimensional accuracy (Ueda et al., 2001; Davies et al., 2007). Particularly under conditions of high cutting speed with minimal material removal, even subtle fluctuations in cutting temperature (typically ±2 °C) can induce microthermal deformations exceeding 50 nm, thereby affecting machining precision and surface quality (Arrazola et al., 2015). Empirical research has demonstrated that excessive cutting temperatures not only accelerate the thermal softening process of tool materials (significantly reducing tool lifespan by 30%–60%), but can also cause microcracks or deformations (2–5 μm) on workpiece surfaces, ultimately impacting product performance and reliability (Hijazi et al., 2011; Sugita et al., 2015). Therefore, accurate monitoring and control of cutting temperature during UPM is vital for improving machining quality and efficiency.

Fig. 1 shows numerous cutting temperature measurement methods which are based on a variety of

✉ Yuan-Liu CHEN, yuanliuchen@zju.edu.cn
Yuan-Liu CHEN, https://orcid.org/0000-0002-1641-051X

Received Mar. 6, 2025; Revision accepted Apr. 17, 2025;
Crosschecked June 3, 2025; Online first Aug. 8, 2025

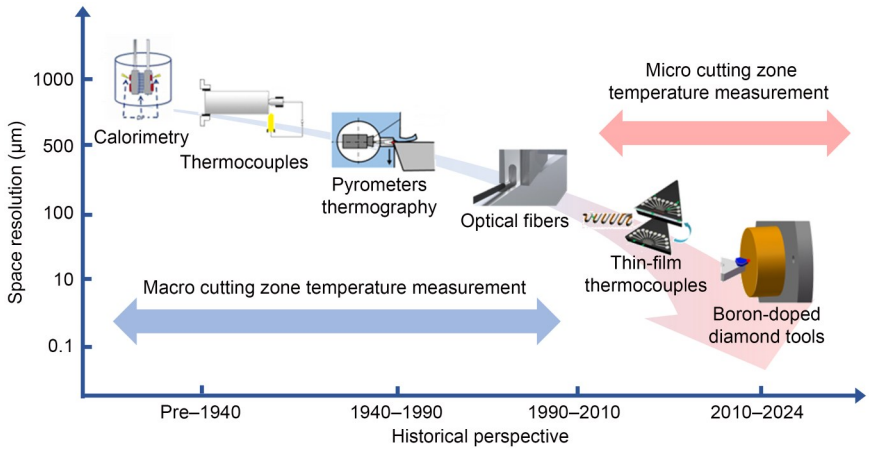

Fig. 1 Historical overview of cutting temperature measurement methods for machining processes (reprinted from (Armendia et al., 2010; Li et al., 2019; Saelzer et al., 2020; Teti et al., 2022; Huang and Yan, 2023; Yan et al., 2023; Song et al., 2024), with permission from Elsevier, from (Yip et al., 2022; Liu et al., 2024b), with permission from Springer, and from (Cichosz et al., 2023), with permission from MDPI)

principles (Tagawa et al., 2003; Armendia et al., 2010; Teti et al., 2022; Yip et al., 2022; Huang and Yan, 2023; Yan et al., 2023; Song et al., 2024). However, temperature measurement in UPM presents inherent challenges. The primary challenge stems from limitations in spatial resolution, since conventional sensing systems struggle to achieve better than 20 μm resolution in micro-scale cutting zones; this is a critical constraint given that heat generation often occurs within 2–5 μm interaction volumes at tool–workpiece interfaces (Huang and Yan, 2023). Compounding this issue, existing systems exhibit temporal latencies exceeding 100 ms in dynamic thermal monitoring, causing significant lag in observing the microsecond-scale thermal transience characteristics associated with nano-scale material removal processes (Herbert, 1926). Thermocouple-based methodologies, which maintain dominance in micro-scale applications, are fundamentally constrained by contact resistance variations (±3%–5% measurement uncertainty) and thermal inertia effects that distort rapid thermal transients (Bono and Ni, 2002). This limitation persists even in advanced micro-thermocouple configurations, where thermal crosstalk between adjacent junctions can alter temperature gradients by 8%–12% (Davies et al., 2003). Infrared thermography circumvents these physical contact issues but faces an insurmountable spatial resolution barrier (≥15 μm) in nanomachining applications, as caused by diffraction limits of mid-infrared wavelengths (3–5 μm spectral range) (Casto et al., 1994). This resolution deficit becomes particularly problematic when monitoring tool-chip interfaces during the diamond turning of optical materials, where thermal boundary layers are often <10 μm thick (Thompson, 1798; Boothroyd, 1963).

Recent advancements in sensor technology, optical measurement techniques, and new materials have led to the emergence of novel temperature measurement methods (Chinchanikar and Choudhury, 2014; Wang et al., 2016). These new technologies enhance measurement accuracy and real-time capabilities while enabling stable measurement in complex cutting environments. Micro-scale sensor technology, tool-integrated sensors, and self-sensing tools have demonstrated prowess in UPM applications (Basti et al., 2007; Hoffmann et al., 2007). These techniques enable real-time monitoring of micro-zone temperature variations during cutting, aiding the understanding of thermodynamic behavior during machining. Furthermore, they establish a foundation for optimizing processing techniques, extending tool life, and improving machining accuracy (Uhlmann et al., 2021).

This review summarizes and examines current cutting temperature measurement methods, with in-depth analysis of various methods' advantages, limitations, and applications. Our review further introduces two recent innovations in cutting temperature measurement for UPM: micro-sensor integration and self-sensing tools, which enable real-time thermal monitoring at cutting edges. Additionally, prospective research directions and potential impacts of these temperature measurement technologies are examined, particularly with regard to atomic and close-to-atomic scale manufacturing

(ACSM), and the convergence of advanced sensing methods, artificial intelligence (AI) technology, and cyber-physical integration. By synthesizing current research and analyzing emerging trends in cutting temperature monitoring, we establish a comprehensive reference to facilitate future innovations that increase machining quality, prolong tool service life, and improve production efficiency.

2 Overview of cutting temperature measurement methods

Accurate cutting temperature monitoring in UPM demands methodologies that can resolve microscale temperature gradients under 10 μm, while also possessing high sensitivity and rapid responsiveness (Guimarães et al., 2022). In Fig. 2, existing temperature monitoring techniques are shown, which are bifurcated into two domains according to their heat transfer mechanisms. Thermal conduction-based methods utilize embedded sensor networks to make direct thermal equilibration measurements, whereas radiation-based methods make non-contact measurements of surface thermal emissions (Xu et al., 2020; Núñez-Cascajero et al., 2021). Each paradigm presents tradeoffs in terms of spatial-temporal resolution and accuracy, as dictated by fundamental physical constraints.

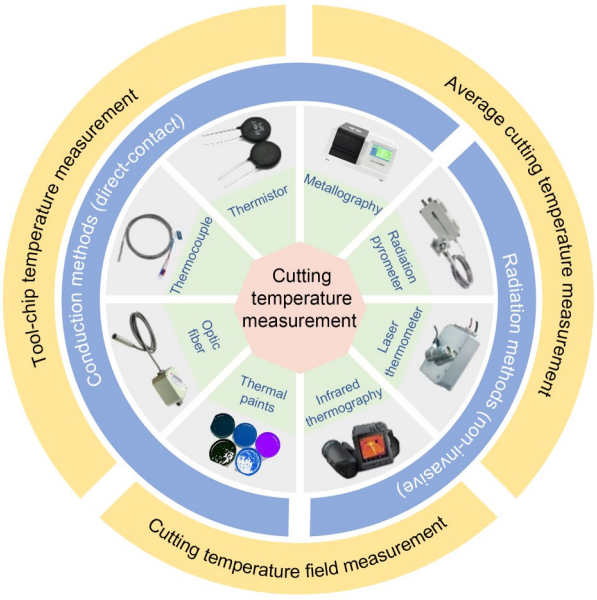

Fig. 2 Cutting temperature measurement methods in machining processes, divided by heat transfer mechanisms

2.1 Thermal conduction methods

Direct-contact thermometry remains foundational in thermal analysis for machining. Thermocouples leveraging thermoelectric principles form the basis of 75% of industrial implementations, according to NIST (National Institute of Standards and Technology, USA) surveys (Komanduri and Hou, 2001). These techniques exploit material-dependent Seeback coefficients (3–80 μV/℃ range) through three operational phases: (1) thermal equilibration between the measurement junction and the cutting zone; (2) electromotive force (EMF) generation proportional to temperature differentials; (3) signal conditioning for noise reduction. The temporal response (τ=300–500 ms) and spatial resolution (500–1000 μm) of these systems are fundamentally constrained by the sensor's thermal mass and heat transfer path geometries (Damarla and Kundu, 2011).

2.1.1 Natural thermocouples

As shown in Fig. 3, natural (tool-work) thermocouple configurations utilize the machining tool and workpiece as inherent thermocouple electrodes. Temperature-dependent EMF generation at the cutting interface enables thermal monitoring, specifically by measuring the voltage between electrically isolated points (Astakhov and Outeiro, 2019). Moura et al. (2015) demonstrated this approach in titanium alloy milling operations using WC-Co tooling, achieving 5 mV/℃ sensitivity across the range of 200–600 ℃. Zhang et al. (2018) proposed an enhanced implementation incorporating high-impedance signal conditioning circuits, attaining 0.2 ℃ resolution during flood-cooled AISI 1045 steel turning experiments (Fig. 4).

While offering simplicity in implementation, this technique has technical limitations that constrain its application. First, material compatibility restrictions limit viable tool-workpiece combinations to those exhibiting stable Seeback coefficients ($|\Delta S|$<5% over 200–600 ℃), as only 12% of common pairs meet this criterion according to data from the ASM Handbook (Bhirud and Gawande, 2017). Furthermore, system recalibration becomes mandatory when altering either the tool substrate (e.g., transitioning from cemented carbide to ceramic tools) or workpiece alloys, which adds significant downtime. Additionally, the inherent thermal inertia of bulk tool-workpiece systems restricts the temporal resolution to >500 ms sampling intervals, which effectively filters out transient thermal fluctuations

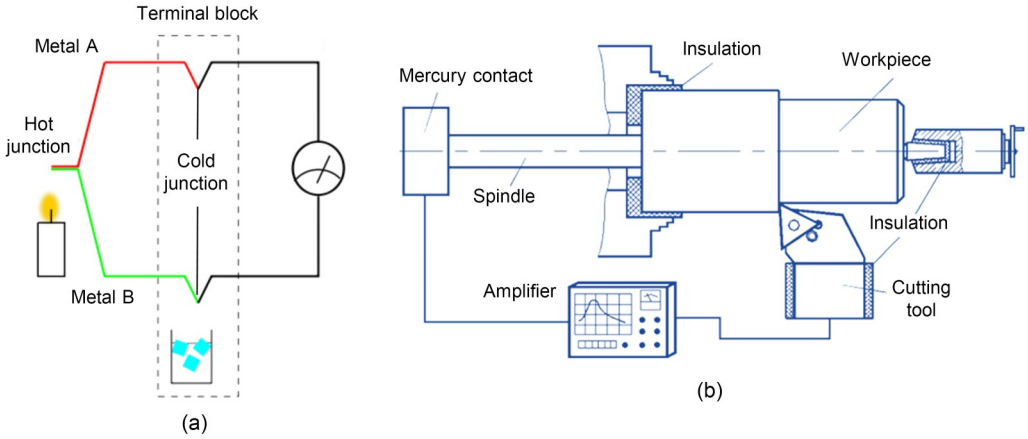

Fig. 3 Schematic of the principle and setup of the tool-work thermocouple method: (a) principle; (b) setup. Reprinted from (Astakhov and Outeiro, 2019), Copyright 2019, with permission from Springer

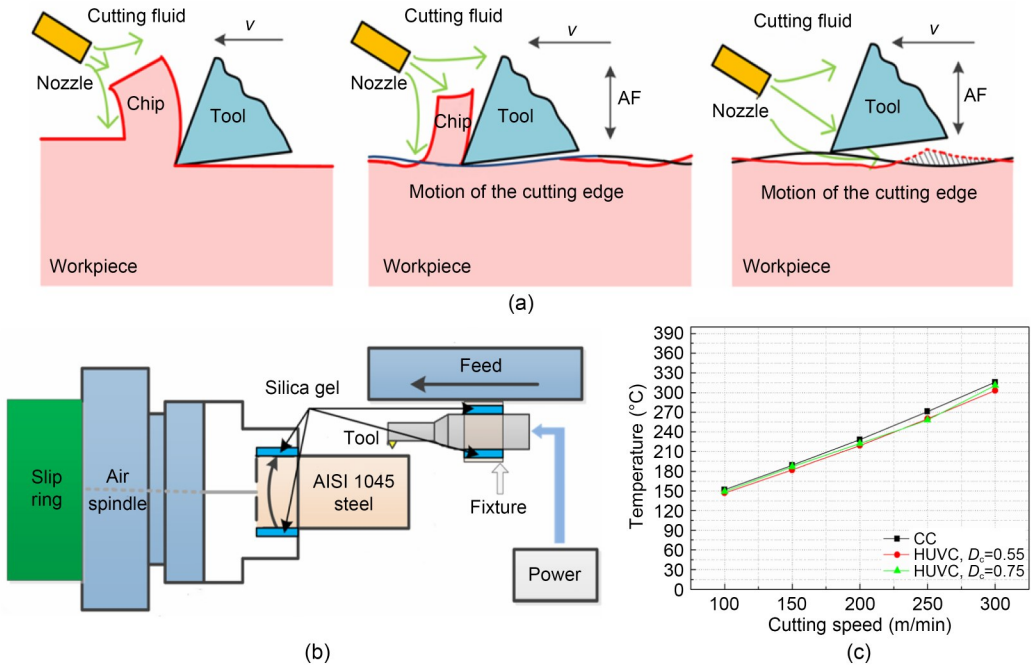

Fig. 4 Cutting temperature measurement using the tool-work thermocouple method under different cooling conditions: (a) schematic representation of cooling conditions; (b) cutting experiment setup; (c) cutting temperature curves. *v* is the cutting speed; AF is the chip thickness; CC is the conventional cutting; HUVC is the high-speed ultrasonic vibration cutting; D_c is the depth of cut. Reprinted from (Zhang et al., 2018), Copyright 2018, with permission from Springer

that are critical for micromachining process analysis. These collective constraints limit natural thermocouple applications to primarily macro-scale cutting operations with stable thermal regimes.

2.1.2 Embedded thermocouples

Cutting tools with integrated calibrated thermocouples enable localized temperature measurements across extreme ranges (−200 to 900 °C) at 50–80 μV/°C sensitivity (Augspurger et al., 2019). As shown in Fig. 5, insulated thermocouple junctions are integrated into tool or workpiece structures through mechanical fixation with dielectric spacers. Embedded thermocouples can be inserted into tools or workpieces for single-point or multi-point temperature monitoring (Chen et al., 2017).

Fig. 6 presents a K-type thermocouple embedded in AISI M2 steel tools via laser-drilled 0.8 mm channels, which captured (680±15) °C peak temperatures

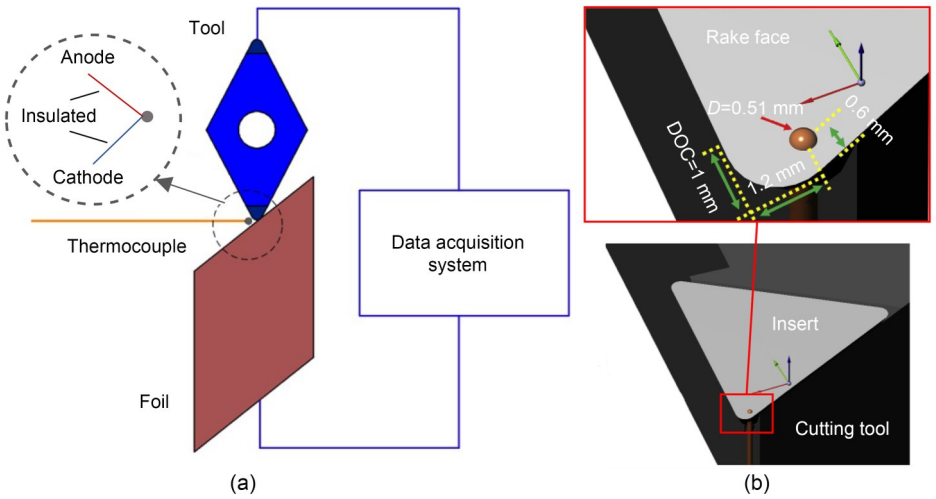

Fig. 5 Schematic representation of the embedded thermocouple method: (a) working principle; (b) embedding structure. *D* is the diameter of tool nose; DOC is the depth of cut. Reprinted from (Chen et al., 2017), Copyright 2017, with permission from Elsevier

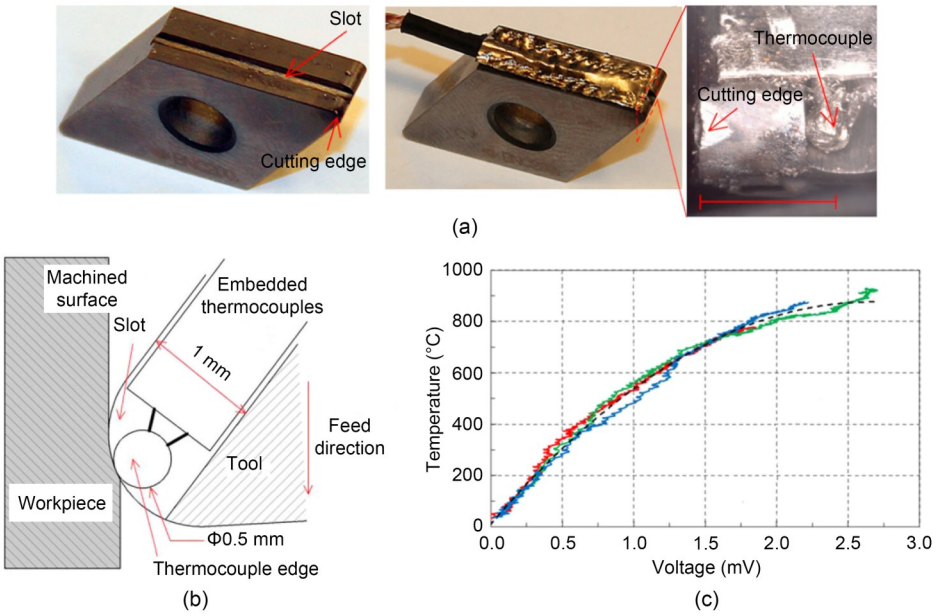

Fig. 6 Cutting temperature monitoring during continuous dry turning of 4140 steels: (a) cutting tool with embedded thermocouples; (b) schematic representation of the embedding; (c) cutting temperature measurement results. Reprinted from (Chen et al., 2017), Copyright 2017, with permission from Elsevier

during continuous dry turning of 4140 steels. Post-process scanning electron microscope (SEM) analysis revealed sensor-induced microcracks within 50 μm of bore surfaces, reducing flank wear resistance by 22% compared to ordinary tools (Chen et al., 2017). Bagherzadeh and Budak (2018) applied the methodology on the rake face in polycrystalline cubic boron nitride (PCBN) tools, comparing the effects of flood cooling on Ti-6Al-4V and Inconel 718 machining temperatures. The 7 °C repeatability data revealed an 18% greater temperature reduction in titanium versus nickel alloys, which was attributed to phase-stabilized heat transfer in γ-strengthened superalloys. Additionally, rotational machining challenges have been partially addressed through wireless telemetry systems, such as the Bluetooth-enabled platform of Campidelli et al. (2019) (Fig. 7), which achieved 100 Hz sampling rates during AISI D2 steel face milling at 120 m/min cutting speed.

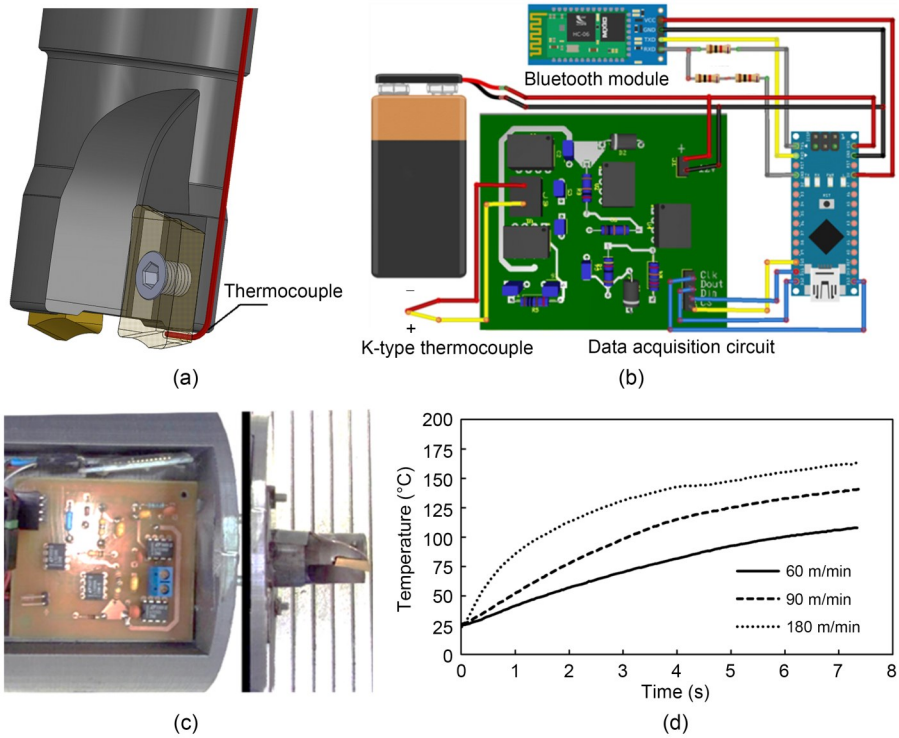

Fig. 7 Cutting temperature measurement system with wireless signal transmission functionality: (a) milling cutter with implanted thermocouple; (b) data acquisition system; (c) tool holder; (d) cutting temperatures for different cutting speed values. Reprinted from (Campidelli et al., 2019), Copyright 2019, with permission from Springer

This system also correlated the radial depth of cut variations (0.5–2.0 mm) with 85–210 °C thermal transients in Al 2024-T3 alloys, exhibiting 120 ms latency and 0.5% packet loss under a spindle speed of 1000 r/min.

Despite the wide range of applications for embedded thermocouples, there exist persistent technical barriers that merit examination. (1) Spatial resolution degradation occurs as thermocouple-tool edge offsets exceed 500 μm in micro-machining configurations, significantly impacting measurement fidelity (Grzesik, 2017). (2) Implementation complexity escalates when advanced tool materials like silicon nitride ceramics or tungsten carbide composites are used, with integration into sensors often inducing stress concentrations that can reduce tool life by 20%–30% (Masek et al., 2021). (3) The embedded sensors' thermal mass perturbs natural heat dissipation patterns, causing up to 18% deviation in tool-chip interface temperature readings. (4) Maintaining reliable electrical insulation between the sensor and tool body remains technically challenging, particularly under high-frequency vibrations (>5 kHz), which are common in precision machining (Brito et al., 2015).

2.1.3 Supplementary cutting temperature measurement methods

In addition to thermal conduction methods utilizing thermoelectric instruments, several supplementary measurement techniques exist:

(1) Fiber-optic thermometry has emerged as a principal method for extreme temperature environments, leveraging single-crystal sapphire fibers to detect temperature-dependent optical transmission shifts at 0.15 nm/°C sensitivity. This technique demonstrates particular efficacy in aerospace component machining, maintaining ±1.5 °C accuracy under 800–1300 °C conditions while resisting electromagnetic interference. However, it also necessitates precision six-axis optical alignment systems with 50 nm positioning repeatability, resulting in 15000–25000 USD peripheral equipment costs that restrict broader industrial deployment (Han et al., 2020).

(2) Metallurgical phase transformation analysis enables retrospective thermal assessment through material characterization. By evaluating post-process martensitic transformation thresholds (in the 250–400 °C critical range), this method enables indirect quantification of

thermal exposure in hardened steel components. Nevertheless, this approach has inherent limitations, including >50 ℃ thermal resolution thresholds, protracted 8–12 h sample preparation cycles involving vacuum mounting, and ion-beam polishing requirements; these constraints preclude real-time process monitoring (da Silva and Wallbank, 1999).

(3) Thermochromic paint coatings, employing functional nanomaterials like cobalt-doped zinc oxide nanoparticles, have been proposed for semi-quantitative thermal visualization. These coatings undergo reversible chromatic transitions across 30–300 ℃ operational ranges, enabling rapid thermal history mapping on complex geometries. Practical implementation, however, has encountered ±20 ℃ measurement uncertainty thresholds, and requires hybrid verification through infrared thermography or embedded micro thermocouples to achieve production-grade accuracy (Kato and Fujii, 1996; Yoo et al., 2020).

2.2 Thermal radiation methods

The evolution of non-invasive thermal monitoring has driven significant developments in radiation-based thermometry for machining applications. These techniques exploit the fundamental relationship between thermal emission spectra and material temperature, which is governed by Planck's radiation law. During machining processes, the tool-workpiece interaction zone emits characteristic infrared radiation with intensity proportional to the fourth power of absolute temperature (Stefan-Boltzmann law) (Abukhshim et al., 2005; Tattersall, 2016; Masoudi et al., 2017). Contemporary implementations utilize this physical principle through two primary configurations: (1) single-wavelength radiation pyrometry for discrete point measurement, and (2) multispectral thermographic imaging for two-dimensional thermal field reconstruction (Bartoszuk, 2020; Jakubek et al., 2022).

2.2.1 Radiation pyrometry

Radiation pyrometry involves spectral analysis of electromagnetic radiation emitted from cutting interfaces (Fig. 8) (Han et al., 2020; Richter and Fouad, 2021). This methodology, pioneered by Manav and Chinchanikar (2018) for metal cutting analysis, underwent critical refinement by Ueda et al. (1992) through the integration of germanium-doped photodetectors. While offering non-contact operational advantages,

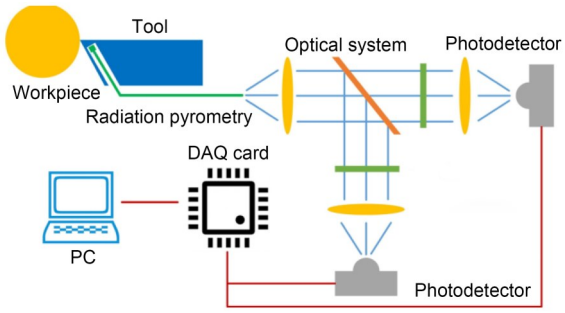

Fig. 8 Schematic diagram of cutting temperature monitoring using radiation pyrometry. DAQ is the data acquisition. Reprinted from (Han et al., 2020), Copyright 2020, with permission from Elsevier

conventional single-channel systems have spatial resolution constraints (typically >50 μm spot size), and yield area-averaged temperature values rather than true interfacial measurements (the contact behavior within the tool-chip interface) (Al Huda et al., 2002). Furthermore, dynamic variations in surface emissivity (ε=0.1–0.9 for metallic surfaces under oxidation) introduce ±7.2% temperature measurement uncertainty per 0.1 deviation in emissivity (Leonidas et al., 2022).

Recent techniques address these challenges with multi-spectral detection. Saelzer et al. (2020) developed a dual-wavelength pyrometry system (InAs detectors, 1.5–2.5 μm spectral range) that effectively decouples emissivity effects through intensity ratio analysis (Fig. 9). This configuration achieved ±0.5 ℃ accuracy in dry grinding applications. Moreover, Zhao et al. (2018) showcased an improved prototype which extended measurable temperatures to 1100 ℃ through optimized optical filtering, albeit with humidity-induced signal attenuation above 85% relative humidity (RH). In nickel-based superalloy machining, Díaz-Álvarez et al. (2017) demonstrated a 250–1200 ℃ measurement range using two-color pyrometry with 0.2 ms response time during Inconel 718 turning (Fig. 10a). Kelly et al. (2021) developed a near-infrared (0.9–1.7 μm) system which further enhanced dynamic response characteristics, maintaining ±93% stability during interrupted cutting with 20 m/s cutting velocities. As shown in Figs. 10b and 10c, Urgoiti et al. (2018) developed a synchronized pyrometer-thermocouple configuration for thermal monitoring during the grinding of GG-30 cast iron, reducing grinding temperature measurement error by 60%.

Despite these improvements, three critical operational constraints persist: (1) the mandatory exclusion of

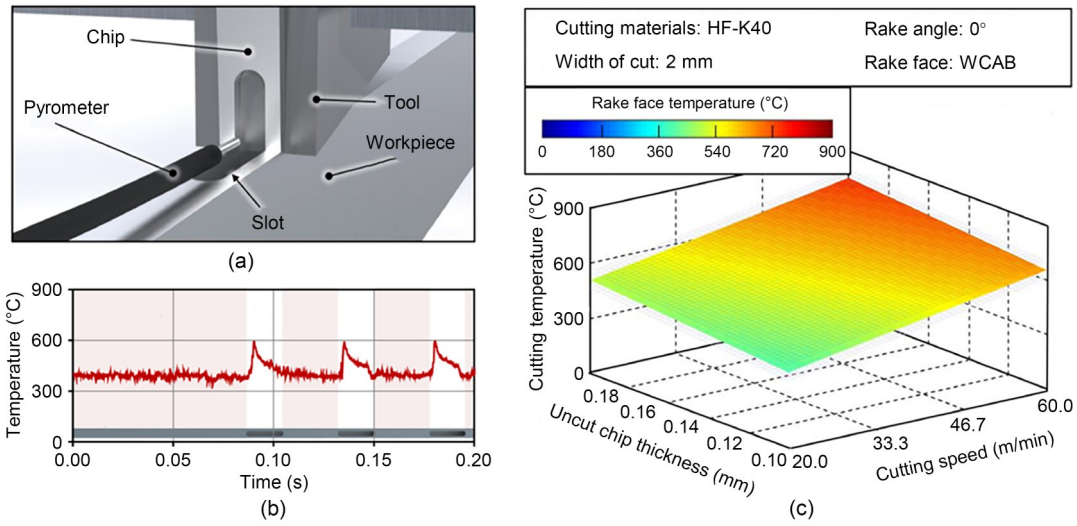

Fig. 9 Schematic representation and experimental results using a radiation pyrometer to measure cutting temperature of HF-K40: (a) experimental setup; (b) temperature measurement results; (c) rake face temperature with cutting speed and uncut chip thickness. WCAB is the wet compressed air blasted. Reprinted from (Saelzer et al., 2020), Copyright 2020, with permission from Elsevier

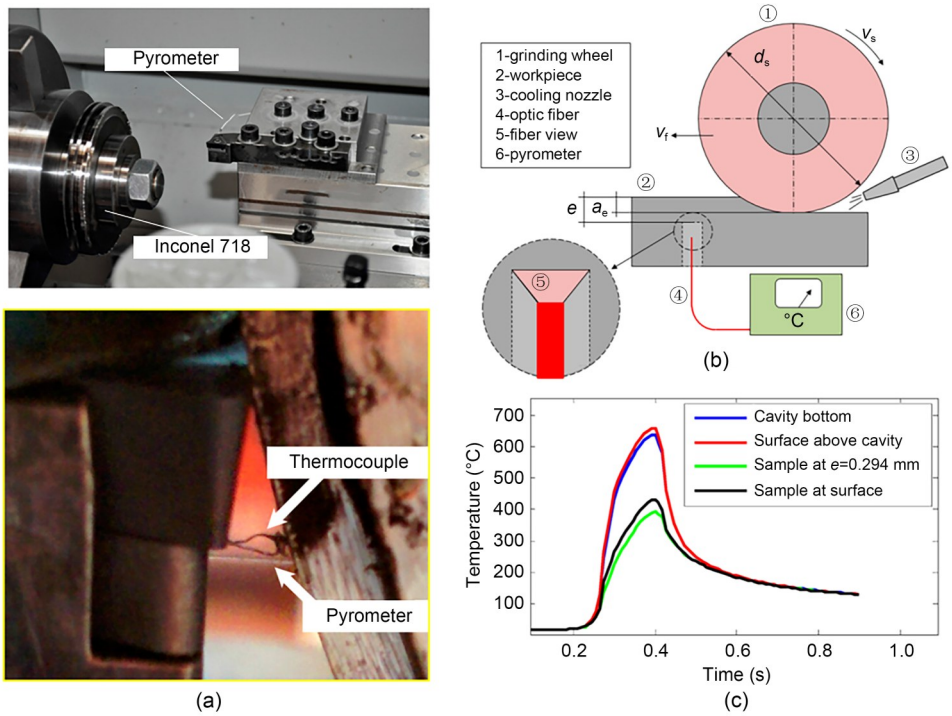

Fig. 10 (a) Setup using a two-color pyrometer to measure the cutting temperature of Inconel 718 (reprinted from (Díaz-Álvarez et al., 2017), Copyright 2017, with permission from MDPI); (b) experimental setup; (c) experimental and simulated temperatures during the grinding process (reprinted from (Urgoiti et al., 2018), Copyright 2018, with permission from MDPI). v_s is the cutting speed; v_f is the feed speed; d_s is the workpiece diameter; a_e is the depth of cut; e is the distance between the sensors and cutting zone. References to color refer to the online version of this figure

cutting fluids to prevent optical path contamination and emissivity alteration; (2) the strategic sensor positioning with >30° elevation angle to avoid chip obstruction; (3) the necessity of in-situ emissivity calibration through controlled heating trials prior to machining (Li TX et al., 2022; Wang et al., 2023).

2.2.2 Infrared thermography

Infrared thermography, developed from the foundational work of Knight and Boothroyd (2005), enables non-invasive thermal mapping of critical machining regions, including primary shear zones and tool-chip interfaces. This methodology employs advanced infrared imaging systems—typically mercury cadmium telluride (MCT) detectors or indium antimonide (InSb) focal plane arrays—to quantify two-dimensional temperature distributions through spectral radiance measurements (Abukhshim et al., 2006; Feng et al., 2015). This technique relies on the calibrated conversion of detected infrared radiation (2–5 μm wavelength range) to temperature via the Stefan-Boltzmann relationship, which requires precise knowledge of the surface emissivity (ε) and environmental transmissivity (Aspinwall et al., 2013; Fernandes et al., 2016).

Experimental work has demonstrated the method's versatility across diverse machining scenarios. For instance, Soler et al. (2018) used an FLIR SC7600 infrared camera (640×512 resolution, 30 Hz frame rate) to monitor Ti-6Al-4V orthogonal cutting processes (Fig. 11), successfully resolving 80–550 °C temperature gradients at tool-chip interfaces while tracking chip formation dynamics through thermal signatures. Thakare and Nordgren (2015) extended this approach to dry turning of AISI 4340 steel, correlating infrared-measured steady-state temperature profiles (200–450 °C) with finite element simulations within 12% deviation margins. Additionally, Heigel et al. (2017) showed that TiAlN-coated tools reduced interfacial temperatures in titanium alloy machining by 25% compared to uncoated counterparts through infrared thermographic analysis, quantitatively demonstrating a reduction in friction (Fig. 12).

While eliminating physical sensor interference is infrared thermography's principal advantage, three technical constraints limit its widespread implementation. First, the nature of the indirect measurement necessitates inverse heat transfer calculations that introduce millisecond-scale computational delays (Manav and Chinchanikar, 2018). Second, dynamic emissivity variations ($\Delta\varepsilon$=±0.15 during chip oxidation) combined with intermittent chip obstructions create 15%–25% measurement uncertainty during continuous operations (Sun et al., 2017). Third, the requirement for high-end cameras (50000–150000 USD) with cryogenic cooling systems hinders integration into production-scale machining environments (Saez-de-Buruaga et al., 2018). However, recent advancements in multi-spectral lock-in

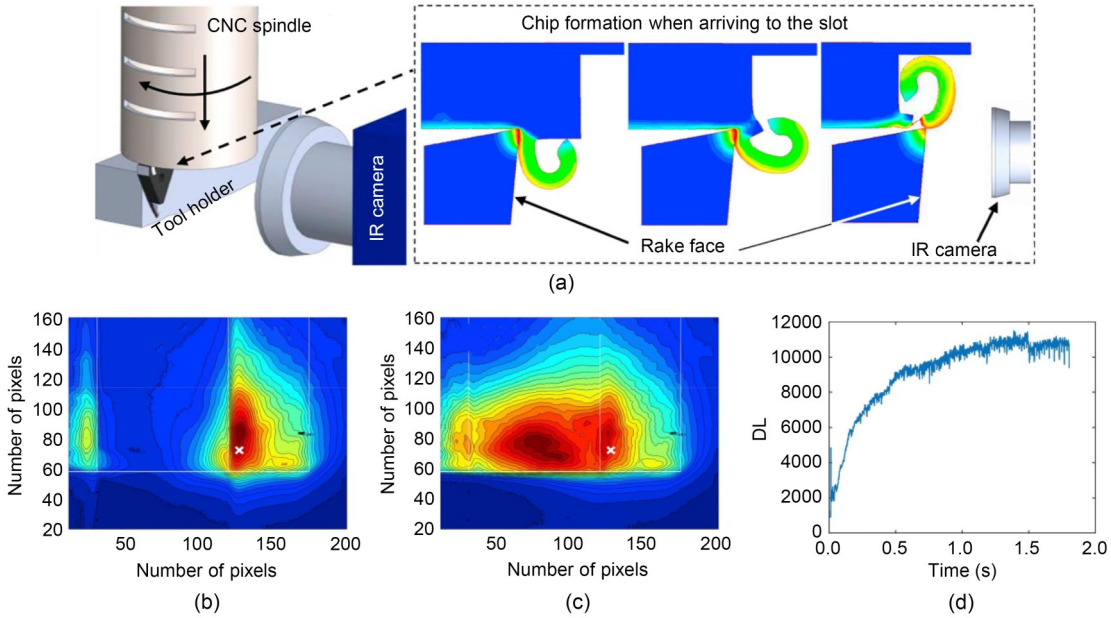

Fig. 11 Measuring of the rake face temperature of the tool during dry orthogonal cutting using thermography: (a) installation of the infrared (IR) thermometer with respect to the tool rake face; (b) thermography of the tool rake face during cutting of the workpiece; (c) thermography of the tool rake face when cutting the air; (d) digital level (DL) versus time of the highlighted pixel of the overhang. CNC is the computer numerical control. Reprinted from (Soler et al., 2018), Copyright 2018, with permission from Elsevier

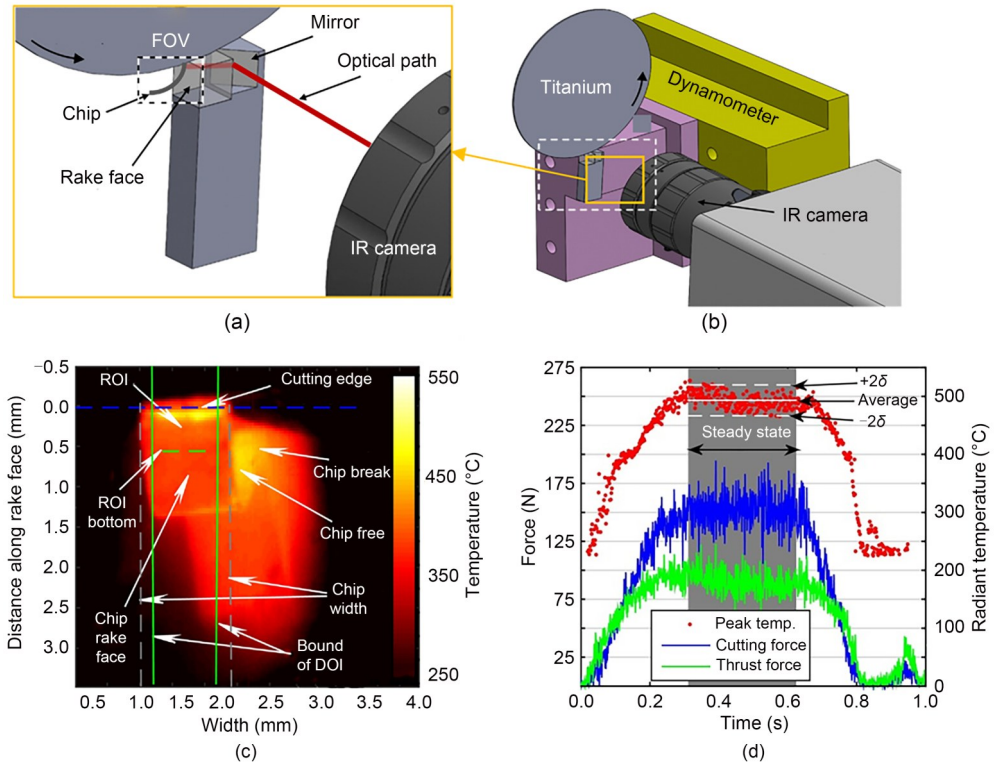

Fig. 12 Cutting temperature measurement during orthogonal cutting of titanium alloys with TiAlN-coated carbide tools employing infrared thermography: (a) experimental setup used to measure the radiant temperature of the tool-chip interface; (b) zoomed-in version; (c) example images from thermal cameras; (d) cutting and thrust forces and the peak temperature in the region of interest. FOV is the field of view; ROI is the region of interest; DOI is the depth of investigation; δ is the error bar. Reprinted from (Heigel et al., 2017), Copyright 2017, with permission from Elsevier

thermography have partially addressed these limitations, achieving ±2 °C accuracy in milling applications through phase-sensitive signal processing (Valiorgue et al., 2013).

3 Micro-zone temperature measurement methods for UPM

In UPM processes, thermal energy generation is predominantly localized within micro/nano-scale interaction zones near tool-workpiece interfaces, typically spanning 0.01–10 μm (Ramesh et al., 2003; Li et al., 2015). Conventional thermometric approaches like infrared thermography (spatial resolution >15 μm) and embedded thermocouples (thermal time constant >100 ms) prove inadequate for resolving the sub-micron thermal gradient characteristics of UPM processes (Attia and Kops, 1993; Chen et al., 2011). Fig. 13 illustrates emerging high-resolution thermal monitoring strategies specifically engineered for UPM, especially

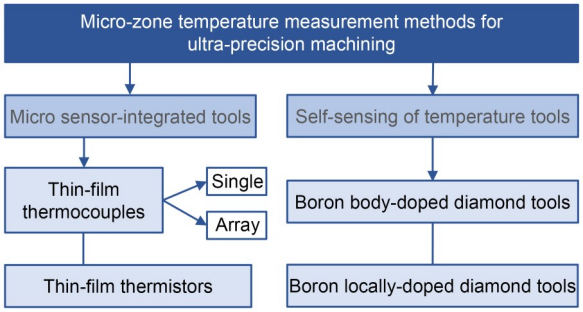

Fig. 13 Micro-zone temperature measurement methods in UPM processes, divided into categories

for single-point diamond cutting (Li JD et al., 2019; Li TX et al., 2021; Liu et al., 2024a; Polte et al., 2025; Xu et al., 2025).

3.1 Micro-scale sensor-integrated tools

The shift towards sensor-integrated cutting tools addresses spatial resolution limitations through direct integration within cutting edges. Modern microfabrication techniques enable deposition of sub-10 μm sensing

elements onto single-crystal diamond tool substrates, achieving localized temperature measurement with <1 μm positional accuracy (Guo et al., 2010; Han et al., 2012; Babu et al., 2014). These integrated systems provide real-time thermal feedback from cutting zones, which was previously inaccessible to macroscopic sensors.

3.1.1 Thin-film thermocouples

Thin-film thermocouples (TFTCs) have emerged as principal sensing elements for micro-zone cutting temperature monitoring in UPM. Fabricated through magnetron sputtering or electron beam evaporation, these 200–500 nm-thick sensor arrays demonstrate sub-millisecond response characteristics when deposited on tool rake/flank faces (Fig. 14) (Chen QN et al., 2023). Their minimal thermal mass (1–3 nJ/K) ensures negligible disturbance to cutting mechanics while enabling operation under cutting fluid immersion. Venkatasubramanian et al. (2001)'s seminal work on Pt-Au TFTCs revealed how quantum confinement effects altered Seeback coefficients by 18%–22% at <50 nm film thicknesses. Subsequent advancements by Cui et al. (2018) validated TFTC functionality in actual cutting environments, recording 250–450 °C interfacial temperatures during steel machining. That same year, Huang Y et al. (2018) utilized TFTC sensors to study the working mechanisms of micro-machining systems.

Recent work has employed microwave plasma chemical vapor deposition (MPCVD) to deposit NiCr/NiSi TFTC arrays on diamond tools, achieving 0.5 °C resolution during aluminum alloy turning with 95% signal correlation to theoretical models (Lian et al., 2023; Sharma et al., 2023). Furthermore, TFTC array configurations (Figs. 15 and 16) enable multi-point thermal mapping through strategic sensor placement. Li LW et al. (2013) and Li TX et al. (2020) developed

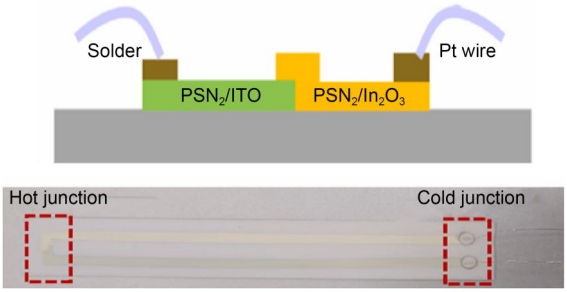

Fig. 14 Fabrication procedure of the K-type TFTC. PSN_2 is the phosphorus and sulfur nitride; ITO is the indium tin oxide. Reprinted from (Chen QN et al., 2023), Copyright 2023, with permission from Elsevier

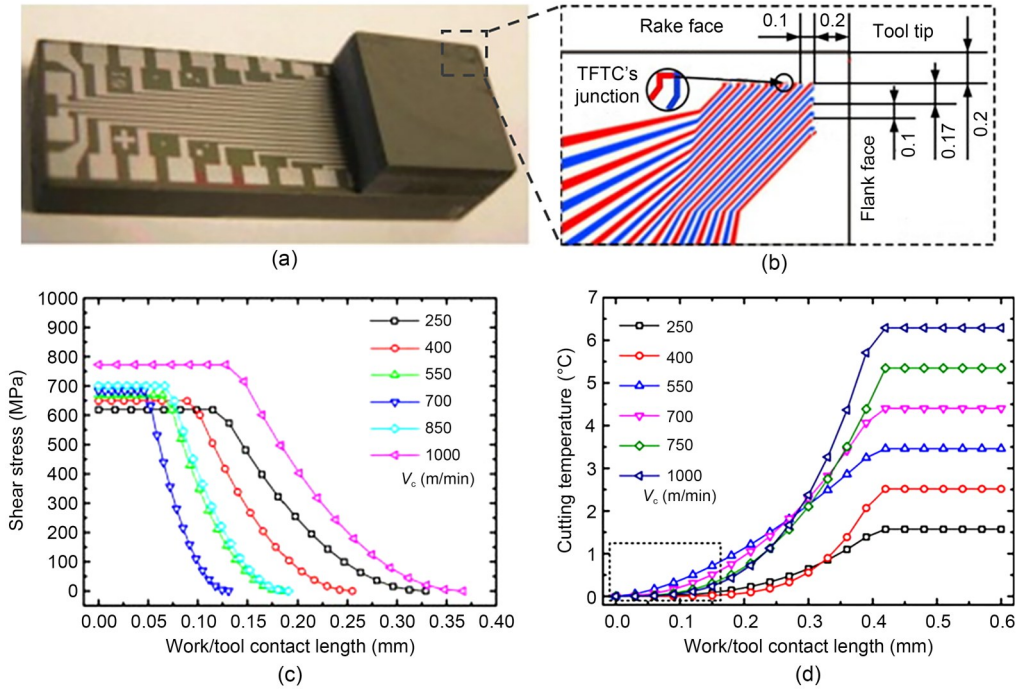

Fig. 15 PCBN insert with embedded micro-TFTCs (a), TFTC localization layout (unit: mm) (b), and shear stress (c) and cutting temperature (d) distributions on the cutting interfaces. V_c is the cutting speed. Reprinted from (Li et al., 2013), Copyright 2013, with permission from Elsevier

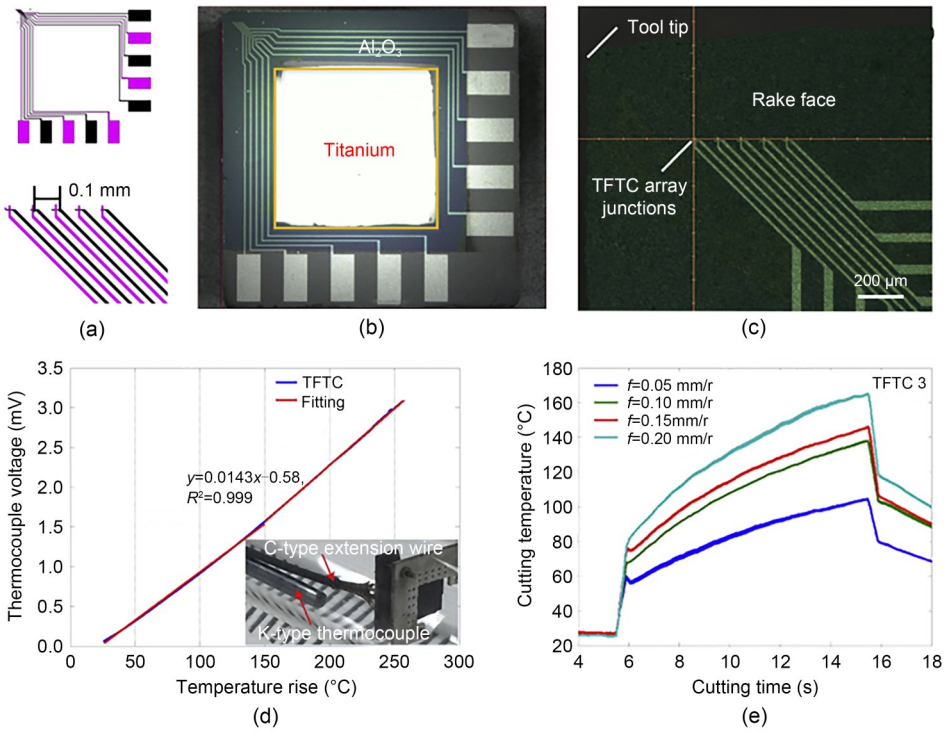

Fig. 16 Temperature monitoring of the tool-chip interface using built-in TFTCs: (a) TFTC localization layout; (b) PCBN insert with embedded micro-TFTCs; (c) zoomed-in view; (d) calibration results of TFTCs; (e) temperature measurement results. *f* is the feed rate. Reprinted from (Li et al., 2020), Copyright 2020, with permission from Elsevier. References to color refer to the online version of this figure

a 4×4 TFTC matrix on rake faces and successfully reconstructed 3D thermal fields with 5 μm spatial resolution, revealing 150–180 °C/mm thermal gradients during copper machining. Nevertheless, critical fabrication challenges persist for TFTC applications, particularly in maintaining 1014 Ω·cm insulation resistance between TFTC junctions and conductive tool substrates. Current solutions employ Al_2O_3/Si_3N_4 dielectric interlayers (200–300 nm thickness) deposited via atomic layer deposition, though pinhole defects (<0.1% area coverage) still cause 5%–8% signal leakage.

3.1.2 Temperature-sensitive semiconductor films

Recently, more approaches utilizing temperature sensor-equipped cutting tools have been proposed, employing temperature-sensitive semiconductor films with boron-doped diamond (BDD). The substituted boron atoms (10^{18}–10^{19} cm^{-3} doping concentration) impart p-type conductivity with −0.5 mV/°C temperature sensitivity through carrier mobility modulation (Yokoya et al., 2005; Mavrin et al., 2008; Wang et al., 2012). Pratas et al. (2021) synthesized a micro-scale BDD film through microwave plasma-assisted chemical vapor deposition, embedding it in the face of the tool rake to achieve online temperature measurement near the tool edge (Fig. 17). This configuration survived over 100 cutting cycles without performance degradation.

However, complications in tool integration remain present: (1) Sensor-integrated tool fabrication faces challenges. Complex multi-step fabrication processes requiring ultra-precise thin-film alignment come with persistent insulation control issues between electrodes and tool substrates. Micron-scale pinhole defects in insulation coatings induce measurable signal distortion through unintended current leakage pathways. (2) There is a fundamental precision-durability paradox. Proximity to cutting edges (<50 μm) enables transient thermal monitoring but accelerates sensor degradation through tool wear mechanisms. Conversely, distal sensor placement (>100 μm) preserves device integrity but introduces critical heat transfer delays that nullify real-time monitoring capabilities (Huang SW et al., 2018). This compromise becomes particularly problematic in diamond tool applications, where periodic edge reconditioning requires complete recalibration of the sensor system following each resharpening cycle.

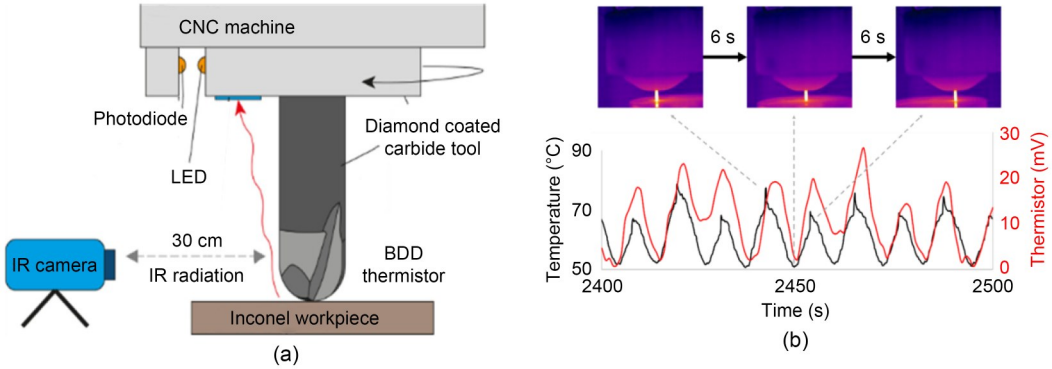

Fig. 17 Micro-zone temperature monitoring during face milling of an Inconel 718 workpiece: (a) overall setup for simultaneous temperature monitoring with an IR camera and BDD thermistor; (b) cutting temperature measurement results. LED is the light-emitting diode. Reprinted from (Pratas et al., 2021), Copyright 2021, with permission from MDPI

The evolution of micro-zone cutting temperature monitoring technologies has driven innovative integration of sensing capabilities into tools themselves. For instance, the pioneering work of Uhlmann et al. (2021) demonstrated that BDD tools (Fig. 18) could inherently function as thermal sensors by leveraging their p-type semiconductive properties, bypassing traditional external sensor requirements. This approach capitalizes on the temperature-dependent resistivity of BDDs, where boron atoms occupying tetrahedral lattice sites create shallow acceptor levels (0.37 eV above the valence band) that govern charge carrier mobility (Koizumi et al., 2001; Ekimov et al., 2006). However, operational limitations to this approach emerge at elevated temperatures (>100 °C), where the thermal energy exceeds the ionization potential of boron impurities, leading to complete carrier excitation and subsequent loss of temperature sensitivity (Lu et al., 2010). Compounding this difficulty, the anisotropic incorporation of boron during the diamond synthesis results in heterogeneous doping densities (5×10^{19}–1×10^{21} cm^{-3}) across crystallographic planes, a phenomenon termed crystallographic orientation-dependent doping disparity (Miao et al., 2018; Sun et al., 2023). Such nonuniform doping generates localized high-resistance zones (10^4–10^6 Ω·μm) that induce parasitic Joule heating, reducing measurement accuracy during continuous machining.

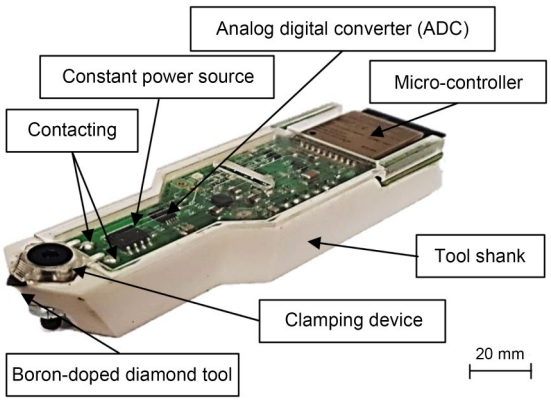

Fig. 18 Cutting temperature measurement system using a BDD tool. Reprinted from (Uhlmann et al., 2021), Copyright 2021, with permission from Elsevier

3.2 Self-sensing of temperature cutting tools

Recent advancements address these limitations through innovative material synthesis. For example, boron (B) and hydrogen (H) co-doping modifies diamond's electronic structure via the formation of B-H complexes, which passivate nitrogen-related trap states and homogenize the carrier distribution (Chen YL et al., 2023; Liu et al., 2025). This synergistic doping enables sustained carrier ionization across 100–300 °C, achieving ±0.1 °C temperature resolution while maintaining the mechanical integrity of the diamond (Fig. 19). Despite these improvements, practical implementation hurdles persist. Bulk BDD tools exhibit inherent thermal inertia (τ=290 ms response time) due to high volumetric heat capacity (1.8 J/(cm^3·K)), limiting their ability to resolve sub-millisecond thermal transients. Furthermore, electrical interactions between conductive workpieces and BDD tools distort temperature readings during metallic machining applications.

In 2024, a breakthrough design employed microwave plasma-assisted confined-layer chemical vapor deposition to fabricate tri-layer diamond tools with spatially engineered functionality (Liu et al., 2024a; Polte et al., 2025). The specific architecture is comprised of an undoped single-crystal diamond substrate

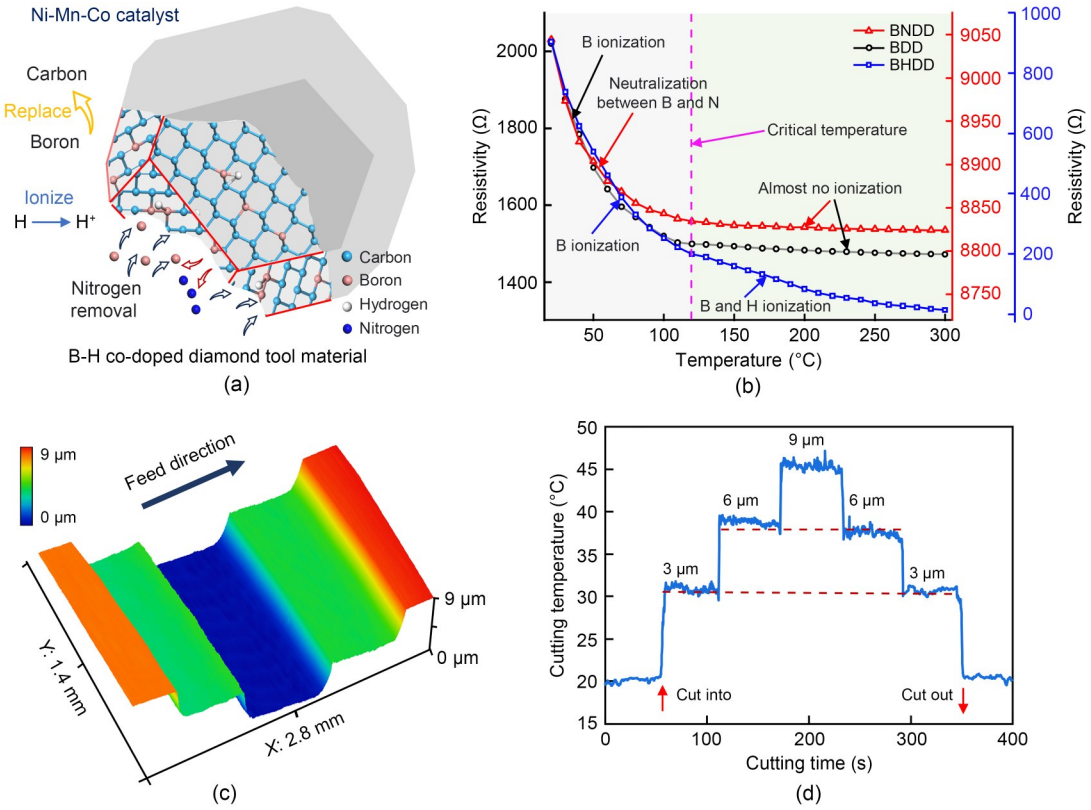

Fig. 19 Mitrogen-removal boron and hydrogen co-doped diamond (BHDD) tool, with self-sensing functionality for micro-zone cutting temperature: (a) growth mechanisms of BHDD samples; (b) heat-sensitive characteristics of the diamond samples from 20 to 300 °C; (c) machined surface profile scanned by a white light interferometer; (d) curve of cutting temperature versus sampling time. BNDD is the boron-doped diamond with nitrogen doping. Reprinted from (Liu et al., 2025), Copyright 2025, with permission from Elsevier

(800 μm), a precisely doped sensing layer (100 μm, 3×10^{20} cm^{-3} boron concentration), and a surface passivation layer (10 μm undoped diamond) (Fig. 20). This configuration reduces thermal mass by 80% compared to conventional BDD tools while achieving 50 ms thermal response times and 0.1 °C resolution. The configuration was validated experimentally during optical component machining, demonstrating a strong correlation between localized temperature fluctuations and the formation of micro-scale surface defects, and highlighting its potential for in-process quality prediction.

4 Future perspectives

There are two emerging paradigms which may influence future research on in-process thermal monitoring during UPM. First, progressive miniaturization of equipment and processes, heading towards atomic-scale manufacturing (sub-nanometer precision), will likely necessitate temperature measurement methods with atomic-level spatial resolution and microkelvin thermal sensitivity. Second, the convergence of AI-driven adaptive sensing systems and internet of things (IoT)-enabled distributed measurement networks will enable real-time monitoring, prediction, and control of machining temperature under dynamic machining conditions.

4.1 Cutting temperature monitoring during atomic and close-to-atomic scale manufacturing

ACSM represents a transformative fabrication paradigm where materials are manipulated at atomic dimensions through controlled removal, transfer, or addition processes. This cutting-edge technology serves as the foundation for developing next-generation devices in computing systems, advanced communication equipment, medical technologies, and novel materials (Gao et al., 2022; Fang et al., 2024) (Fig. 21).

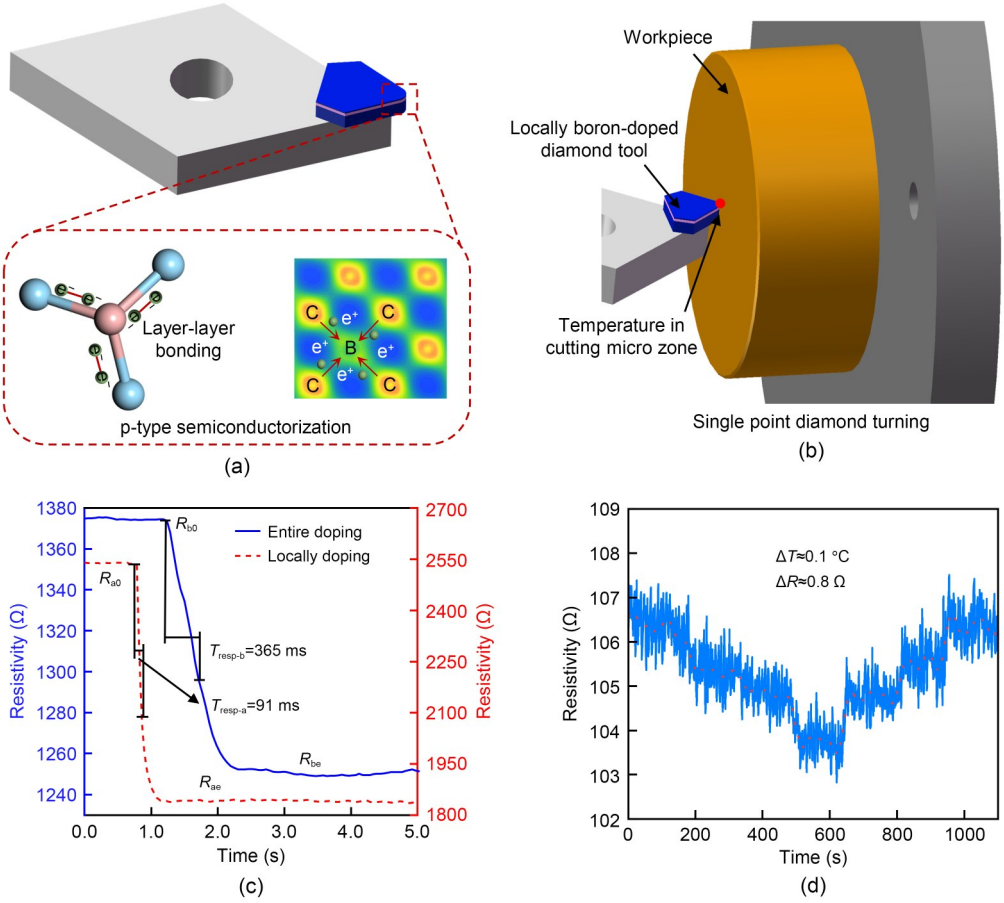

Fig. 20 Locally BDD tool, with functionality for self-sensing of micro-zone cutting temperature: (a) work mechanisms of locally-doped BDD samples; (b) schematic of the setup; (c) thermal response test; (d) temperature resolution test. R_{a0} is the resistivity of locally BDD tool at 20 °C; R_{b0} is the resistivity of entire BDD tool at 20 °C; R_{ae} is the resistivity of locally BDD tool at 50 °C; R_{be} is the resistivity of entire BDD tool at 50 °C; T_{resp-a} is the heating response time of locally BDD tool; T_{resp-b} is the heating response time of entire BDD tool; ΔT is the temperature gradient; ΔR is the variation of tool's resistivity. Reprinted from (Liu et al., 2024b), Copyright 2024, with permission from Springer

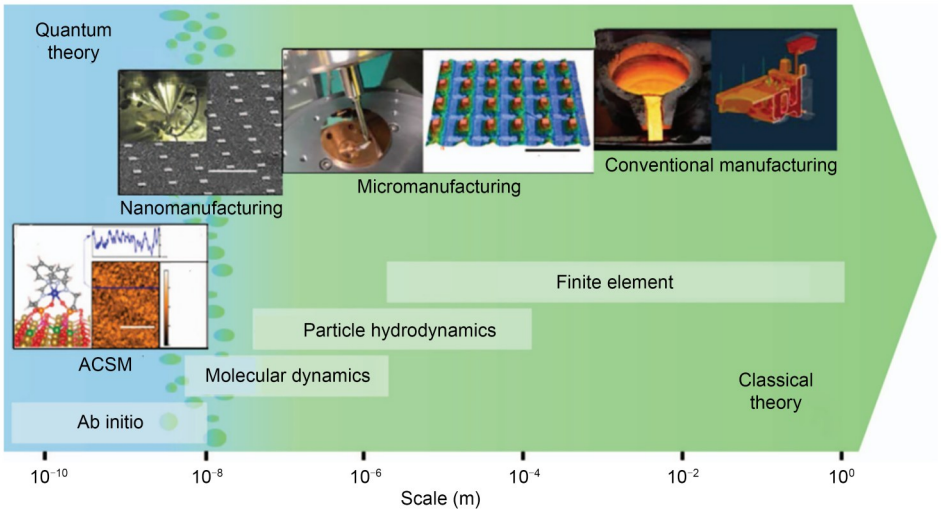

Fig. 21 Length scale map of manufacturing systems, modeling methods, and dominant theories. Reprinted from (Gao et al., 2022), Copyright 2022, with permission from IOP Publishing

However, this technology brings forth unprecedented challenges in thermal monitoring and management, particularly during atomic-scale fabrication processes. The extreme precision required at sub-nanometer scales imposes rigorous demands on temperature measurement methods, necessitating exceptional spatial resolution (sub-nanometer level), ultra-high sensitivity (μK range), and sub-picosecond temporal resolution. These requirements are further complicated by the operational constraints of electron microscopy environments, where most ACSM processes occur; specifically, these include ultrahigh vacuum conditions (10^{-6} to 10^{-8} Pa) and exposure to high-energy electron beams (80–300 keV) (Fang, 2020). Current thermal characterization techniques face fundamental limitations in such scenarios. Conventional contact thermometry suffers from probe-induced surface perturbations, while optical pyrometry becomes impractical under electron beam irradiation. This technological gap underscores the need for novel in-situ thermometric approaches that are compatible with scanning/transmission electron microscope (S/TEM) instrumentation. Recent innovations in self-sensing tool systems demonstrate particular promise, where the machining tool itself functions as an atomic-scale thermal sensor through engineered p-type semiconductorization of diamonds. Such integrated metrology solutions could enable real-time thermal mapping with atomic-scale spatial fidelity while maintaining process integrity under dynamic fabrication conditions.

4.2 Smart sensor networks and IoT

The combination of smart sensor technology and IoT offers novel solutions for temperature measurement (Chen et al., 2018; Al-Naggar et al., 2021). By embedding sensors in cutting tools, workpieces, or machine tools, real-time temperature data can be recorded and transmitted to central processing systems (Fig. 22). IoT applications enable instantaneous wireless transmission of such data, with storage and processing on cloud platforms, reducing the complexity and costs associated with traditional wired sensors and allowing remote monitoring and management. Smart sensors can not only monitor real-time temperature variations in the cutting zone, but also work in conjunction with other sensors (such as vibration and force sensors) to provide multi-dimensional feedback on the machining process. Through IoT technology, manufacturers can remotely access real-time machining data and automatically identify overheating issues or anomalies. With the development of 5G and other wireless communication technologies, the real-time data transmission speed and stability of IoT are increasing, providing more efficient online monitoring and data analysis capabilities for manufacturing.

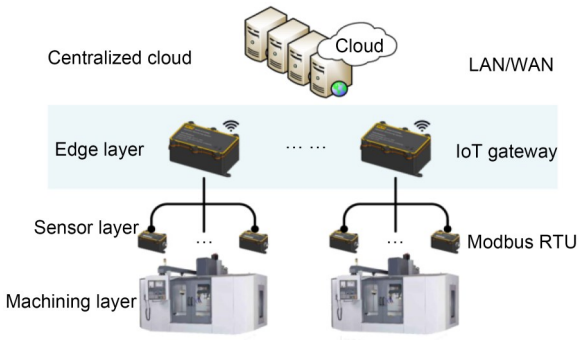

Fig. 22 Overall architecture of an edge-to-cloud based IoT condition monitoring system. LAN/WAN is the local area network/wide area network; RTU is the remote terminal unit. Reprinted from (Li Z et al., 2022), Copyright 2022, with permission from MDPI

4.3 Multimodal data fusion and multi-physics modeling

Prospective studies will likely focus on data fusion technology that establishes closer correlations between various process parameters, improving the accuracy and reliability of temperature measurements (Xu et al., 2021). By integrating cutting temperature with other critical parameters, such as cutting force, vibration, tool wear, and material properties, data fusion technology can deepen understanding of the interactions between temperature and other factors (Fig. 23). Specifically, excessive temperature may lead to material softening and changes in cutting force, while excessive cutting force may cause further temperature increases, creating a complex feedback mechanism. Real-time data fusion enables more accurate assessment of machining states, identification of potential issues, and early warning capabilities. Furthermore, the application of multi-physics modeling technology may enhance the quality of temperature distribution predictions. Traditional thermal conduction models typically only consider thermal effects, while modern multi-physics modeling can simultaneously account for thermal, mechanical, and fluid factors affecting the temperature field, enabling more precise simulations of temperature

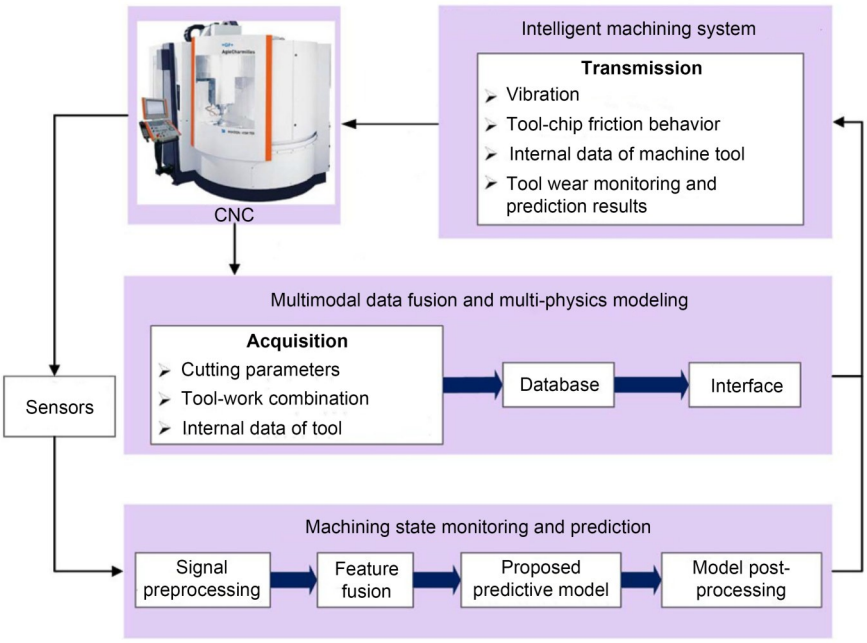

Fig. 23 Diagram of the intelligent monitoring system for machining states to be implemented. Reprinted from (Xu et al., 2021), Copyright 2021, with permission from Elsevier

variations during cutting. For example, the influence of coolant flow on temperature and the frictional heat at the tool-workpiece interface have been incorporated into models (Wang et al., 2021). With improvements in computational power and simulation technology, these models will become more accurate and efficient, serving as indispensable tools for optimizing UPM processes.

4.4 AI-driven predictive thermal control

AI and machine learning technologies can extract valuable patterns from vast temperature data, enhancing the accuracy and reliability of temperature measurement systems (Mishra et al., 2021; Ma and Yu, 2023). By analyzing historical temperature data and current machining conditions, AI systems can automatically predict potential machining issues such as tool wear, excessive cutting, or insufficient cooling when abnormal temperature fluctuations occur. Machine learning algorithms also have the power to optimize temperature control strategies through continuous feedback loops, automatically adjusting machining parameters such as cutting speed, feed rate, and depth of cutting, so as to achieve more precise thermal management and avoid the negative effects of extreme temperatures on machining quality and tool life (Raman and Halam, 2023; Sharma et al., 2024; Si et al., 2024). In the future, with continuous training and optimization of machine learning models, systems will possess more intelligent adaptive capabilities, enabling real-time responses to changes in machining conditions. Moreover, temperature-related machining issues could be predicted and prevented, thereby significantly improving production efficiency and machining accuracy (Fig. 24). The integration of AI could enable temperature measurement systems to not only provide real-time monitoring, but also exert more precise process control through predicted trends in the data.

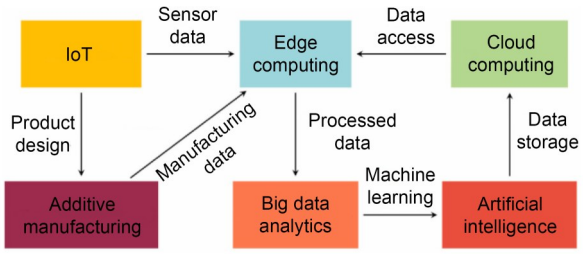

Fig. 24 Different components of Industry 4.0. Reprinted from (Sharma et al., 2024), Copyright 2024, with permission from Elsevier

5 Conclusions

Cutting temperature monitoring technology for UPM plays a crucial role in enhancing machining

accuracy, surface quality, and tool life. This review systematically analyzed in-process cutting temperature measurement methods, outlining their strengths and weaknesses, and discussing avenues for future work, leading to the following main conclusions:

(1) Traditional temperature measurement methods, such as thermocouple techniques and infrared thermography, have shown a notable degree of success in applications. However, they still face challenges in terms of spatial resolution and response speed, and display limited dynamic performance when applied to UPM. Thus, it is difficult for such methods to meet the temperature measurement requirements associated with micro/nano-scale cutting zones.

(2) With the continuous development of miniaturized and integrated sensors, new cutting temperature measurement methods are being rapidly developed. These methods are increasingly recognized as viable solutions to challenges in micro-zone temperature monitoring, real-time feedback, and adaptive control.

(3) The development of smart sensors and IoT technology has enabled real-time data collection and remote monitoring, significantly advancing temperature control capabilities in UPM. By integrating multisensor data and utilizing AI for data analysis, more precise and intelligent temperature control can be achieved, ultimately improving the tool life, reducing the occurrence of machining defects, and optimizing the production efficiency.

Future advancements in in-process thermal monitoring at micro/nano-scale machining zones will likely be driven by two synergistic research trajectories. First, the progressive miniaturization of manufacturing systems towards atomic-scale precision necessitates breakthroughs in thermal measurement and characterization technologies. This scaling paradigm imposes stringent requirements for non-invasive temperature mapping with atomic-level spatial resolution (<0.5 nm) and microkelvin-level thermal sensitivity, and demands fundamental innovation in thermometric methods. Meanwhile, cutting temperature measurement methodologies for UPM will further integrate big data analytics, cloud computing, and smart manufacturing systems. This convergence will likely create a more interconnected and intelligent production environment, where real-time temperature data may be monitored and integrated with other parameter conditions to comprehensively optimize production.

Acknowledgments

This work is supported by the National Natural Science Foundation of China (Nos. 52425505 and U22A20207), the National Key R&D Program of China (No. 2022YFB3403302), and the Zhejiang Provincial Key R&D Program of China (No. 2023C01056).

Author contributions

Shiquan LIU contributed to the methodology, software development and validation, corresponding data processing, and manuscript organization. Yuqi DING contributed to the methodology, software development, and validation. Kaiyang XIA and Hui LI contributed to the methodology, experimental design, and software development. Liang AN and Zhongwei LI assisted in organizing the manuscript. Yuan-Liu CHEN contributed to overall research direction and planning, and reviewed the manuscript.

Conflict of interest

Shiquan LIU, Yuqi DING, Kaiyang XIA, Hui LI, Liang AN, Zhongwei LI, and Yuan-Liu CHEN declare that they have no conflict of interest.

References

Abukhshim NA, Mativenga PT, Sheikh MA, 2005. Investigation of heat partition in high speed turning of high strength alloy steel. *International Journal of Machine Tools and Manufacture*, 45(15):1687-1695. https://doi.org/10.1016/j.ijmachtools.2005.03.008

Abukhshim NA, Mativenga PT, Sheikh MA, 2006. Heat generation and temperature prediction in metal cutting: a review and implications for high speed machining. *International Journal of Machine Tools and Manufacture*, 46(7-8):782-800. https://doi.org/10.1016/j.ijmachtools.2005.07.024

Al Huda M, Yamada K, Hosokawa A, et al., 2002. Investigation of temperature at tool-chip interface in turning using two-color pyrometer. *Journal of Manufacturing Science and Engineering*, 124(2):200-207. https://doi.org/10.1115/1.1455641

Al-Naggar YM, Jamil N, Hassan MF, et al., 2021. Condition monitoring based on IoT for predictive maintenance of CNC machines. *Procedia CIRP*, 102:314-318. https://doi.org/10.1016/j.procir.2021.09.054

Armendia M, Garay A, Villar A, et al., 2010. High bandwidth temperature measurement in interrupted cutting of difficult to machine materials. *CIRP Annals*, 59(1):97-100. https://doi.org/10.1016/j.cirp.2010.03.059

Arrazola PJ, Aristimuno P, Soler D, et al., 2015. Metal cutting experiments and modelling for improved determination of chip/tool contact temperature by infrared thermography. *CIRP Annals*, 64(1):57-60. https://doi.org/10.1016/j.cirp.2015.04.061

Aspinwall DK, Mantle AL, Chan WK, et al., 2013. Cutting temperatures when ball nose end milling γ-TiAl intermetallic

alloys. *CIRP Annals*, 62(1):75-78.
https://doi.org/10.1016/j.cirp.2013.03.007

Astakhov VP, Outeiro J, 2019. Importance of temperature in metal cutting and its proper measurement/modeling. *In*: Davim JP (Ed.), Measurement in Machining and Tribology. Springer, Cham, Switzerland, p.1-47.
https://doi.org/10.1007/978-3-030-03822-9_1

Attia MH, Kops L, 1993. Thermometric design considerations for temperature monitoring in machine tools and CMM structures. *The International Journal of Advanced Manufacturing Technology*, 8(5):311-319.
https://doi.org/10.1007/BF01783615

Augspurger T, Koch M, Klocke F, et al., 2019. Investigation of transient temperature fields in the milling cutter under CO_2 cooling by means of an embedded thermocouple. *Procedia CIRP*, 79:33-38.
https://doi.org/10.1016/j.procir.2019.02.007

Babu R, Raja VP, Kanchana J, et al., 2014. Identification, development and testing of thermal error compensation model for a headstock assembly of CNC turning centre. *International Journal of Engineering and Technology*, 3(2):113-122.
https://doi.org/10.14419/ijet.v3i2.2012

Bagherzadeh A, Budak E, 2018. Investigation of machinability in turning of difficult-to-cut materials using a new cryogenic cooling approach. *Tribology International*, 119:510-520.
https://doi.org/10.1016/j.triboint.2017.11.033

Bartoszuk M, 2020. Thermovision measurements of the tool-chip upper side temperature in turning AISI 321 steel. *Technical Sciences*, 23(1):69-80.
https://doi.org/10.31648/ts.5177

Basti A, Obikawa T, Shinozuka J, 2007. Tools with built-in thin film thermocouple sensors for monitoring cutting temperature. *International Journal of Machine Tools and Manufacture*, 47(5):793-798.
https://doi.org/10.1016/j.ijmachtools.2006.09.007

Bhirud NL, Gawande RR, 2017. Measurement and prediction of cutting temperatures during dry milling: review and discussions. *Journal of the Brazilian Society of Mechanical Sciences and Engineering*, 39(12):5135-5158.
https://doi.org/10.1007/s40430-017-0869-7

Bono M, Ni J, 2002. A method for measuring the temperature distribution along the cutting edges of a drill. *Journal of Manufacturing Science and Engineering*, 124(4):921-923.
https://doi.org/10.1115/1.1511525

Boothroyd G, 1963. Temperatures in orthogonal metal cutting. *Proceedings of the Institution of Mechanical Engineers*, 177(1):789-810.
https://doi.org/10.1243/pime_proc_1963_177_058_02

Brinksmeier E, Lucca DA, Walter A, 2004. Chemical aspects of machining processes. *CIRP Annals*, 53(2):685-699.
https://doi.org/10.1016/S0007-8506(07)60035-3

Brito RF, Carvalho SR, Silva SMMLE , 2015. Experimental investigation of thermal aspects in a cutting tool using COMSOL and inverse problem. *Applied Thermal Engineering*, 86:60-68.
https://doi.org/10.1016/j.applthermaleng.2015.03.083

Campidelli AFV, Lima HV, Abrão AM, et al., 2019. Development of a wireless system for milling temperature monitoring. *The International Journal of Advanced Manufacturing Technology*, 104(1-4):1551-1560.
https://doi.org/10.1007/s00170-019-04088-0

Casto SL, Valvo EL, Piacentini M, et al., 1994. Cutting temperatures evaluation in ceramic tools: experimental tests, numerical analysis and SEM observations. *CIRP Annals*, 43(1):73-76.
https://doi.org/10.1016/S0007-8506(07)62167-2

Chen BT, Wan JF, Celesti A, et al., 2018. Edge computing in IoT-based manufacturing. *IEEE Communications Magazine*, 56(9):103-109.
https://doi.org/10.1109/MCOM.2018.1701231

Chen C, Zhang JF, Wu ZJ, et al., 2011. Real-time measurement of machine tool temperature fields and their effect on machining errors. *Mechanika*, 17(4):413-417.
https://doi.org/10.5755/j01.mech.17.4.572

Chen L, Tai BL, Chaudhari RG, et al., 2017. Machined surface temperature in hard turning. *International Journal of Machine Tools and Manufacture*, 121:10-21.
https://doi.org/10.1016/j.ijmachtools.2017.03.003

Chen QN, Zhang P, Liu K, et al., 2023. Polymer-derived ceramic thin-film thermocouples for high temperature measurements. *Ceramics International*, 49(19):31248-31254.
https://doi.org/10.1016/j.ceramint.2023.07.072

Chen YL, Liu SQ, Chen XZ, et al., 2023. Self-sensing of cutting temperature in single point diamond turning by a boron-doped diamond tool. *CIRP Annals*, 72(1):81-84.
https://doi.org/10.1016/j.cirp.2023.04.048

Chinchanikar S, Choudhury SK, 2014. Evaluation of chip-tool interface temperature: effect of tool coating and cutting parameters during turning hardened AISI 4340 steel. *Procedia Materials Science*, 6:996-1005.
https://doi.org/10.1016/j.mspro.2014.07.170

Cichosz P, Karolczak P, Waszczuk K, 2023. Review of cutting temperature measurement methods. *Materials*, 16(19):6365.
https://doi.org/10.3390/ma16196365

Cui YX, Liu QY, Wang LH, et al., 2018. Research on milling temperature measuring tool embedded with NiCr/NiSi thin film thermocouple. *Procedia CIRP*, 72:1457-1462.
https://doi.org/10.1016/j.procir.2018.03.109

da Silva MB, Wallbank J, 1999. Cutting temperature: prediction and measurement methods—a review. *Journal of Materials Processing Technology*, 88(1-3):195-202.
https://doi.org/10.1016/S0924-0136(98)00395-1

Damarla SK, Kundu P, 2011. Classification of unknown thermocouple types using similarity factor measurement. *Sensors & Transducers*, 124:11-18.

Davies MA, Cao Q, Cooks AL, et al., 2003. On the measurement and prediction of temperature fields in machining AISI 1045 steel. *CIRP Annals*, 52(1):77-80.
https://doi.org/10.1016/S0007-8506(07)60535-6

Davies MA, Ueda T, M'Saoubi R, et al., 2007. On the measurement of temperature in material removal processes. *CIRP Annals*, 56(2):581-604.
https://doi.org/10.1016/j.cirp.2007.10.009

Díaz-Álvarez J, Tapetado A, Vázquez C, et al., 2017. Temperature measurement and numerical prediction in machining

Inconel 718. *Sensors*, 17(7):1531. https://doi.org/10.3390/s17071531

Ekimov EA, Sidorov VA, Rakhmanina AV, et al., 2006. High-pressure synthesis and characterization of superconducting boron-doped diamond. *Science and Technology of Advanced Materials*, 7(1):S2-S6. https://doi.org/10.1016/j.stam.2006.03.004

Fan ZY, Hu XC, Gao RX, 2022. Indirect measurement methods for quality and process control in nanomanufacturing. *Nanomanufacturing and Metrology*, 5(3):209-229. https://doi.org/10.1007/s41871-022-00148-4

Fang FZ, 2020. Atomic and close-to-atomic scale manufacturing: perspectives and measures. *International Journal of Extreme Manufacturing*, 2:030201. https://doi.org/10.1088/2631-7990/aba495

Fang FZ, Zhang XD, Gao W, et al., 2017. Nanomanufacturing—perspective and applications. *CIRP Annals*, 66(2):683-705. https://doi.org/10.1016/j.cirp.2017.05.004

Fang FZ, Lai M, Wang JS, et al., 2022. Nanometric cutting: mechanisms, practices and future perspectives. *International Journal of Machine Tools and Manufacture*, 178:103905. https://doi.org/10.1016/j.ijmachtools.2022.103905

Fang FZ, Luo XC, Dai GL, et al., 2024. Atomic and close-to-atomic scale manufacturing: the fundamental technology of manufacturing III. *In*: Tolio T (Ed.), CIRP Novel Topics in Production Engineering: Volume 1. Springer, Cham, Switzerland, p.315-360. https://doi.org/10.1007/978-3-031-54034-9_9

Feng Y, Zheng L, Wang ML, et al., 2015. Research on cutting temperature of work-piece in milling process based on WPSO. *The International Journal of Advanced Manufacturing Technology*, 79(1-4):427-435. https://doi.org/10.1007/s00170-015-6808-9

Fernandes MGA, Fonseca EMM, Natal RJ, 2016. Thermal analysis during bone drilling using rigid polyurethane foams: numerical and experimental methodologies. *Journal of the Brazilian Society of Mechanical Sciences and Engineering*, 38(7):1855-1863. https://doi.org/10.1007/s40430-016-0560-4

Gao J, Luo XC, Fang FZ, et al., 2022. Fundamentals of atomic and close-to-atomic scale manufacturing: a review. *International Journal of Extreme Manufacturing*, 4(1):012001. https://doi.org/10.1088/2631-7990/ac3bb2

Gao W, Chen YL, Lee KW, et al., 2013. Precision tool setting for fabrication of a microstructure array. *CIRP Annals*, 62(1):523-526. https://doi.org/10.1016/j.cirp.2013.03.013

Gao W, Ibaraki S, Donmez MA, et al., 2023. Machine tool calibration: measurement, modeling, and compensation of machine tool errors. *International Journal of Machine Tools and Manufacture*, 187:104017. https://doi.org/10.1016/j.ijmachtools.2023.104017

Grzesik W, 2017. Chapter nine–heat in metal cutting. *In*: Grzesik W (Ed.), Advanced Machining Processes of Metallic Materials (Second Edition). Elsevier, p.163-182. https://doi.org/10.1016/B978-0-444-63711-6.00009-0

Guimarães BMP, da Silva Fernandes CM, de Figueiredo DA, et al., 2022. Cutting temperature measurement and prediction in machining processes: comprehensive review and future perspectives. *The International Journal of Advanced Manufacturing Technology*, 120(5-6):2849-2878. https://doi.org/10.1007/s00170-022-08957-z

Guo QJ, Yang JG, Wu H, 2010. Application of ACO-BPN to thermal error modeling of NC machine tool. *The International Journal of Advanced Manufacturing Technology*, 50(5-8):667-675. https://doi.org/10.1007/s00170-010-2520-y

Han J, Wang LP, Wang HT, et al., 2012. A new thermal error modeling method for CNC machine tools. *The International Journal of Advanced Manufacturing Technology*, 62(1-4):205-212. https://doi.org/10.1007/s00170-011-3796-2

Han JH, Cao KW, Xiao L, et al., 2020. In situ measurement of cutting edge temperature in turning using a near-infrared fiber-optic two-color pyrometer. *Measurement*, 156:107595. https://doi.org/10.1016/j.measurement.2020.107595

Heigel JC, Whitenton E, Lane B, et al., 2017. Infrared measurement of the temperature at the tool–chip interface while machining Ti–6Al–4V. *Journal of Materials Processing Technology*, 243:123-130. https://doi.org/10.1016/j.jmatprotec.2016.11.026

Herbert EG, 1926. The measurement of cutting temperatures. *Proceedings of the Institution of Mechanical Engineers*, 110(1):289-329. https://doi.org/10.1243/pime_proc_1926_110_018_02

Hijazi A, Sachidanandan S, Singh R, et al., 2011. A calibrated dual-wavelength infrared thermometry approach with non-greybody compensation for machining temperature measurements. *Measurement Science and Technology*, 22(2):025106. https://doi.org/10.1088/0957-0233/22/2/025106

Hoffmann L, Müller MS, Krämer S, et al., 2007. Applications of fibre optic temperature measurement. *Proceedings of the Estonian Academy of Sciences. Engineering*, 13(4):363-378. https://doi.org/10.3176/eng.2007.4.09

Huang SW, Tao B, Li JD, et al., 2018. Estimation of the time and space-dependent heat flux distribution at the tool-chip interface during turning using an inverse method and thin film thermocouples measurement. *The International Journal of Advanced Manufacturing Technology*, 99(5-8):1531-1543. https://doi.org/10.1007/s00170-018-2585-6

Huang WH, Yan JW, 2023. Mechanisms of tool-workpiece interaction in ultraprecision diamond turning of single-crystal SiC for curved microstructures. *International Journal of Machine Tools and Manufacture*, 191:104063. https://doi.org/10.1016/j.ijmachtools.2023.104063

Huang Y, Ji JJ, Lee KM, 2018. An improved material constitutive model considering temperature-dependent dynamic recrystallization for numerical analysis of Ti-6Al-4V alloy machining. *The International Journal of Advanced Manufacturing Technology*, 97(9-12):3655-3670. https://doi.org/10.1007/s00170-018-2210-8

Jakubek B, Grochalski K, Rukat W, et al., 2022. Thermovision measurements of rolling bearings. *Measurement*, 189:

110512.
https://doi.org/10.1016/j.measurement.2021.110512

Jawahir IS, Brinksmeier E, M'Saoubi R, et al., 2011. Surface integrity in material removal processes: recent advances. *CIRP Annals*, 60(2):603-626.
https://doi.org/10.1016/j.cirp.2011.05.002

Kato T, Fujii H, 1996. PVD film method for measuring the temperature distribution in cutting tools. *Journal of Engineering for Industry*, 118(1):117-122.
https://doi.org/10.1115/1.2803632

Kelly DL, Scarborough DE, Thurow BS, 2021. A novel multiband plenoptic pyrometer for high-temperature applications. *Measurement Science and Technology*, 32(10):105901.
https://doi.org/10.1088/1361-6501/ac0465

Knight WA, Boothroyd G, 2005. Fundamentals of Metal Machining and Machine Tools. 3rd Edition, CRC Press, Boca Raton, USA, p.112-115.
https://doi.org/10.1201/9780429114243

Koizumi S, Watanabe K, Hasegawa M, et al., 2001. Ultraviolet emission from a diamond pn junction. *Science*, 292(5523):1899-1901.
https://doi.org/10.1126/science.1060258

Komanduri R, Hou ZB, 2001. A review of the experimental techniques for the measurement of heat and temperatures generated in some manufacturing processes and tribology. *Tribology International*, 34(10):653-682.
https://doi.org/10.1016/S0301-679X(01)00068-8

Leonidas E, Ayvar-Soberanis S, Laalej H, et al., 2022. A comparative review of thermocouple and infrared radiation temperature measurement methods during the machining of metals. *Sensors*, 22(13):4693.
https://doi.org/10.3390/s22134693

Li JD, Tao B, Huang SW, et al., 2019. Cutting tools embedded with thin film thermocouples vertically to the rake face for temperature measurement. *Sensors and Actuators A: Physical*, 296:392-399.
https://doi.org/10.1016/j.sna.2019.07.043

Li LW, Li B, Ehmann KF, et al., 2013. A thermo-mechanical model of dry orthogonal cutting and its experimental validation through embedded micro-scale thin film thermocouple arrays in PCBN tooling. *International Journal of Machine Tools and Manufacture*, 70:70-87.
https://doi.org/10.1016/j.ijmachtools.2013.03.005

Li TX, Shi TL, Tang ZR, et al., 2020. Temperature monitoring of the tool-chip interface for PCBN tools using built-in thin-film thermocouples in turning of titanium alloy. *Journal of Materials Processing Technology*, 275:116376.
https://doi.org/10.1016/j.jmatprotec.2019.116376

Li TX, Shi TL, Tang ZR, et al., 2021. Real-time tool wear monitoring using thin-film thermocouple. *Journal of Materials Processing Technology*, 288:116901.
https://doi.org/10.1016/j.jmatprotec.2020.116901

Li TX, Long H, Shi TL, et al., 2022. Cutting temperature measurement using a novel near-infrared two-color pyrometer under dry and wet cutting of Ti-6Al-4V alloy. *Journal of Materials Processing Technology*, 309:117751.
https://doi.org/10.1016/j.jmatprotec.2022.117751

Li Y, Zhao WH, Lan SH, et al., 2015. A review on spindle thermal error compensation in machine tools. *International Journal of Machine Tools and Manufacture*, 95:20-38.
https://doi.org/10.1016/j.ijmachtools.2015.04.008

Li Z, Fei F, Zhang GL, 2022. Edge-to-cloud IIoT for condition monitoring in manufacturing systems with ubiquitous smart sensors. *Sensors*, 22(15):5901.
https://doi.org/10.3390/s22155901

Lian YS, Chen XD, Zhang TY, et al., 2023. Temperature measurement performance of thin-film thermocouple cutting tool in turning titanium alloy. *Ceramics International*, 49(2):2250-2261.
https://doi.org/10.1016/j.ceramint.2022.09.193

Liu SQ, An L, Li H, et al., 2024a. Characterization and optimization of a locally boron-doped diamond tool for self-sensing of cutting temperature. *Nanomanufacturing and Metrology*, 7(1):24.
https://doi.org/10.1007/s41871-024-00243-8

Liu SQ, An L, Chen XZ, et al., 2024b. A locally boron-doped diamond tool for self-sensing of cutting temperature: lower thermal capacity and broader applications. *The International Journal of Advanced Manufacturing Technology*, 135(7-8):3301-3315.
https://doi.org/10.1007/s00170-024-14703-4

Liu SQ, An L, Li H, et al., 2025. Micro-zone cutting temperature measurement using a nitrogen-extracted boron and hydrogen co-doped diamond tool for ultra-precision machining. *International Journal of Machine Tools and Manufacture*, 205:104244.
https://doi.org/10.1016/j.ijmachtools.2024.104244

Lu C, Wang ZL, Xu LF, et al., 2010. The metallicity of B-doped diamond surface by first-principles study. *Diamond and Related Materials*, 19(7-9):824-828.
https://doi.org/10.1016/j.diamond.2010.01.050

Ma QY, Yu HY, 2023, Artificial intelligence-enabled mode-locked fiber laser: a review. *Nanomanufacturing and Metrology*, 6(1):36.
https://doi.org/10.1007/s41871-023-00216-3

Manav O, Chinchanikar S, 2018. Multi-objective optimization of hard turning: a genetic algorithm approach. *Materials Today: Proceedings*, 5(5):12240-12248.
https://doi.org/10.1016/j.matpr.2018.02.201

Masek P, Zeman P, Kolar P, 2021. Cutting temperature measurement in turning of thermoplastic composites using a tool-work thermocouple. *The International Journal of Advanced Manufacturing Technology*, 116(9-10):3163-3178.
https://doi.org/10.1007/s00170-021-07588-0

Masoudi S, Gholami MA, Janghorban IM, et al., 2017. Infrared temperature measurement and increasing infrared measurement accuracy in the context of machining process. *Advances in Production Engineering & Management*, 12(4):353-362.
https://doi.org/10.14743/apem2017.4.263

Mavrin BN, Denisov VN, Popova DM, et al., 2008. Boron distribution in the subsurface region of heavily doped IIb type diamond. *Physics Letters A*, 372(21):3914-3918.
https://doi.org/10.1016/j.physleta.2008.02.064

Miao XY, Chen LC, Ma HA, et al., 2018. Studies on HPHT

synthesis and N defects of N-rich B-doped diamonds. *CrystEngComm*, 20(44):7109-7113. https://doi.org/10.1039/c8ce01146j

Mishra D, Gupta A, Raj P, et al., 2021. Sensor based real-time information for monitoring and control of a manufacturing process. *Engineering Research Express*, 3(2):025040. https://doi.org/10.1088/2631-8695/ac0777

Moura RR, da Silva MB, Machado ÁR, et al., 2015. The effect of application of cutting fluid with solid lubricant in suspension during cutting of Ti-6Al-4V alloy. *Wear*, 332-333: 762-771. https://doi.org/10.1016/j.wear.2015.02.051

Núñez-Cascajero A, Tapetado A, Vargas S, et al., 2021. Optical fiber pyrometer designs for temperature measurements depending on object size. *Sensors*, 21(2):646. https://doi.org/10.3390/s21020646

Polte J, Hocke T, Thißen K, et al., 2025. Fundamental investigations on temperature development in ultra-precision turning. *The International Journal of Advanced Manufacturing Technology*, 136(5-6):2455-2491. https://doi.org/10.1007/s00170-024-14846-4

Pratas S, Silva EL, Neto MA, et al., 2021. Boron doped diamond for real-time wireless cutting temperature monitoring of diamond coated carbide tools. *Materials*, 14(23):7334. https://doi.org/10.3390/ma14237334

Raman R, Halam R, 2023. Embedded sensor networks for smart industrial automation and control systems. The 7th International Conference on I-SMAC (IoT in Social, Mobile, Analytics and Cloud), p.1016-1021. https://doi.org/10.1109/I-SMAC58438.2023.10290456

Ramesh R, Mannan MA, Poo AN, 2003. Thermal error measurement and modelling in machine tools. Part I. Influence of varying operating conditions. *International Journal of Machine Tools and Manufacture*, 43(4):391-404. https://doi.org/10.1016/S0890-6955(02)00263-8

Richter T, Fouad NA, 2021. Guidelines for Thermography in Architecture and Civil Engineering: Theory, Application Areas, Practical Implementation. Birkhäuser, Basel, Switzerland. https://doi.org/10.1515/9783035622683

Saelzer J, Berger S, Iovkov I, et al., 2020. In-situ measurement of rake face temperatures in orthogonal cutting. *CIRP Annals*, 69(1):61-64. https://doi.org/10.1016/j.cirp.2020.04.021

Saez-de-Buruaga M, Soler D, Aristimuño PX, et al., 2018. Determining tool/chip temperatures from thermography measurements in metal cutting. *Applied Thermal Engineering*, 145:305-314. https://doi.org/10.1016/j.applthermaleng.2018.09.051

Sharma A, Kulasegaram S, Brousseau E, et al., 2023. Investigation of nanoscale scratching on copper with conical tools using particle-based simulation. *Nanomanufacturing and Metrology*, 6(1):5. https://doi.org/10.1007/s41871-023-00179-5

Sharma D, Kumar A, Tyagi N, et al., 2024. Towards intelligent industrial systems: a comprehensive survey of sensor fusion techniques in IIoT. *Measurement: Sensors*, 32:100944. https://doi.org/10.1016/j.measen.2023.100944

Si SM, Mu DQ, Si ZK, 2024. Intelligent tool wear prediction based on deep learning PSD-CVT model. *Scientific Reports*, 14(1):20754. https://doi.org/10.1038/s41598-024-71795-4

Soler D, Aristimuño PX, Saez-de-Buruaga M, et al., 2018. New calibration method to measure rake face temperature of the tool during dry orthogonal cutting using thermography. *Applied Thermal Engineering*, 137:74-82. https://doi.org/10.1016/j.applthermaleng.2018.03.056

Song CS, Xiang DH, Zhao B, et al., 2024. Improving wear resistance and machining performance of diamond tools in ferrous metals cutting: a review. *Journal of Materials Processing Technology*, 334:118618. https://doi.org/10.1016/j.jmatprotec.2024.118618

Sugita N, Ishii K, Furusho T, et al., 2015. Cutting temperature measurement by a micro-sensor array integrated on the rake face of a cutting tool. *CIRP Annals*, 64(1):77-80. https://doi.org/10.1016/j.cirp.2015.04.079

Sun KY, Lu TJ, He MY, et al., 2023. Characterization on the occurrence state of nitrogen getter Ti in HPHT grown synthetic diamond crystals. *Journal of Crystal Growth*, 622:127390. https://doi.org/10.1016/j.jcrysgro.2023.127390

Sun YJ, Sun J, Li JF, 2017. Modeling and experimental study of temperature distributions in end milling Ti6Al4V with solid carbide tool. *Proceedings of the Institution of Mechanical Engineers, Part B: Journal of Engineering Manufacture*, 231(2):217-227. https://doi.org/10.1177/0954405415577553

Tagawa M, Kato K, Ohta Y, 2003. Response compensation of temperature sensors: frequency-domain estimation of thermal time constants. *Review of Scientific Instruments*, 74(6): 3171-3174. https://doi.org/10.1063/1.1571948

Tattersall GJ, 2016. Infrared thermography: a non-invasive window into thermal physiology. *Comparative Biochemistry and Physiology Part A: Molecular & Integrative Physiology*, 202:78-98. https://doi.org/10.1016/j.cbpa.2016.02.022

Teti R, Mourtzis D, D'Addona DM, et al., 2022. Process monitoring of machining. *CIRP Annals*, 71(2):529-552. https://doi.org/10.1016/j.cirp.2022.05.009

Thakare A, Nordgren A, 2015. Experimental study and modeling of steady state temperature distributions in coated cemented carbide tools in turning. *Procedia CIRP*, 31:234-239. https://doi.org/10.1016/j.procir.2015.03.024

Thompson B, 1798. IV. An inquiry concerning the source of the heat which is excited by friction. *Philosophical Transactions*, 88:80-102. https://doi.org/10.1098/rstl.1798.0006

Ueda T, Yamada K, Sugita T, 1992. Measurement of grinding temperature of ceramics using infrared radiation pyrometer with optical fiber. *Journal of Engineering for Industry*, 114(3):317-322. https://doi.org/10.1115/1.2899798

Ueda T, Hosokawa A, Oda K, et al., 2001. Temperature on flank face of cutting tool in high speed milling. *CIRP Annals*, 50(1):37-40. https://doi.org/10.1016/S0007-8506(07)62065-4

Uhlmann E, Polte J, Polte M, et al., 2021. Boron-doped

monocrystalline diamond as cutting tool for temperature measurement in the cutting zone. *Procedia CIRP*, 101: 258-261. https://doi.org/10.1016/j.procir.2021.02.026

Urgoiti L, Barrenetxea D, Sánchez JA, et al., 2018. On the influence of infra-red sensor in the accurate estimation of grinding temperatures. *Sensors*, 18(12):4134. https://doi.org/10.3390/s18124134

Valiorgue F, Brosse A, Naisson P, et al., 2013. Emissivity calibration for temperatures measurement using thermography in the context of machining. *Applied Thermal Engineering*, 58(1-2):321-326. https://doi.org/10.1016/j.applthermaleng.2013.03.051

Venkatasubramanian R, Siivola E, Colpitts T, et al., 2001. Thin-film thermoelectric devices with high room-temperature figures of merit. *Nature*, 413(6856):597-602. https://doi.org/10.1038/35098012

Wang BC, Tao F, Fang XD, et al., 2021. Smart manufacturing and intelligent manufacturing: a comparative review. *Engineering*, 7(6):738-757. https://doi.org/10.1016/j.eng.2020.07.017

Wang HJ, Sun J, Li JF, et al., 2016. Evaluation of cutting force and cutting temperature in milling carbon fiber-reinforced polymer composites. *The International Journal of Advanced Manufacturing Technology*, 82(9-12): 1517-1525. https://doi.org/10.1007/s00170-015-7479-2

Wang KY, Steeds J, Li ZH, 2012. Photoluminescence studies of 515.8 nm, 533.5 nm and 580 nm centres in electron irradiated type IIa diamond. *Diamond and Related Materials*, 25:29-33. https://doi.org/10.1016/j.diamond.2012.02.012

Wang ZT, Dai JM, Yang S, 2023. The development of a multi-spectral pyrometer for achievable true temperature field measurements of the explosion flame. *Measurement Science and Technology*, 34(6):065501. https://doi.org/10.1088/1361-6501/acc047

Xu JY, Li C, Chen M, et al., 2020. On the analysis of temperatures, surface morphologies and tool wear in drilling CFRP/Ti6Al4V stacks under different cutting sequence strategies. *Composite Structures*, 234:111708. https://doi.org/10.1016/j.compstruct.2019.111708

Xu XW, Wang JW, Zhong BF, et al., 2021. Deep learning-based tool wear prediction and its application for machining process using multi-scale feature fusion and channel attention mechanism. *Measurement*, 177:109254. https://doi.org/10.1016/j.measurement.2021.109254

Xu ZJ, Zhang GQ, Zhang JB, et al., 2025. Wear mechanisms of diamond tools and their material basis in machining iron-based materials. *Precision Engineering*, 93:110-152. https://doi.org/10.1016/j.precisioneng.2025.01.004

Yan B, Chen N, Zhu Y, et al., 2023. Instantaneous formation of covalently bonded diamond–graphite–graphene with synergistic properties. *International Journal of Machine Tools and Manufacture*, 193:104087. https://doi.org/10.1016/j.ijmachtools.2023.104087

Yip WS, To S, Zhou HT, 2022. Current status, challenges and opportunities of sustainable ultra-precision manufacturing. *Journal of Intelligent Manufacturing*, 33(8):2193-2205. https://doi.org/10.1007/s10845-021-01782-3

Yokoya T, Nakamura T, Matsushita T, et al., 2005. Origin of the metallic properties of heavily boron-doped superconducting diamond. *Nature*, 438(7068):647-650. https://doi.org/10.1038/nature04278

Yoo S, Dugasani SR, Jeon S, et al., 2020. Chroma-hue controllable color and thermocolor-added deoxyribonucleic acid films. *Thin Solid Films*, 706:138072. https://doi.org/10.1016/j.tsf.2020.138072

Zhang XY, Lu ZH, Peng ZL, et al., 2018. Development of a tool-workpiece thermocouple system for comparative study of the cutting temperature when high-speed ultrasonic vibration cutting Ti-6Al-4V alloys with and without cutting fluids. *The International Journal of Advanced Manufacturing Technology*, 96(1-4):237-246. https://doi.org/10.1007/s00170-018-1600-2

Zhao JF, Liu ZQ, Wang B, et al., 2018. Cutting temperature measurement using an improved two-color infrared thermometer in turning Inconel 718 with whisker-reinforced ceramic tools. *Ceramics International*, 44(15):19002-19007. https://doi.org/10.1016/j.ceramint.2018.07.142